

# Beyond Diagonal RIS-Aided Wireless Communications Systems: State-of-the-Art and Future Research Directions

Omar Maraqa, Majid H. Khoshafa, *Senior Member, IEEE*, Olutayo O. Oyerinde, *Senior Member, IEEE*, and Telex M. N. Ngatched, *Senior Member, IEEE*

## CONTENTS

**Abstract**—Integrating beyond diagonal reconfigurable intelligent surface (BD-RIS) into wireless communications systems has attracted significant interest due to its transformative potential in enhancing system performance. This survey provides a comprehensive analysis of BD-RIS technology, examining its modeling, structural characteristics, and network integration while highlighting its advantages over traditional diagonal RIS (D-RIS). Specifically, we review various BD-RIS modeling approaches, including multiport network theory, graph theory, and matrix theory, and emphasize their application in diverse wireless scenarios. The survey also covers BD-RIS’s structural diversity, including different scattering matrix types, transmission modes, intercell architectures, and circuit topologies, showing their flexibility in improving network performance. We delve into the potential applications of BD-RIS, such as enhancing wireless coverage, improving physical layer security (PLS), enabling multi-cell interference cancellation, improving precise sensing and localization, and optimizing channel manipulation. Further, we explore BD-RIS architectural development, providing insights into new configurations focusing on channel estimation, optimization, performance analysis, and circuit complexity perspectives. Additionally, we investigate the integration of BD-RIS with emerging wireless technologies, such as millimeter-wave and terahertz communications, integrated sensing and communications, mobile edge computing, and other cutting-edge technologies. These integrations are pivotal in advancing the capabilities and efficiency of future wireless networks. Finally, the survey identifies key challenges, including channel state information estimation, interference modeling, and phase-shift designs, and outlines future research directions. The survey aims to provide valuable insights into BD-RIS’s potential in shaping the future of wireless communications systems.

**Index Terms**—Beyond diagonal RIS (BD-RIS), diagonal RIS (D-RIS), 6G, RIS 2.0, non-diagonal BD-RIS, BD-RIS modeling, BD-RIS classification, BD-RIS applications, BD-RIS architectural development, physical layer security (PLS), millimeter wave (mmWave), terahertz (THz), integrated sensing and communications (ISAC), mobile edge computing (MEC), radar communications, simultaneous wireless information and power transfer (SWIPT), ultra-reliable low-latency communications (URLLC), rate splitting multiple access (RSMA), non-orthogonal multiple access (NOMA), wideband systems, large-scale systems.

O. Maraqa, M. H. Khoshafa, and T. M. N. Ngatched are with the Department of Electrical and Computer Engineering, McMaster University, Hamilton, ON L8S 4L8, Canada (e-mail: {maraqao@mcmaster.ca, khoshafm@mcmaster.ca, and ngatched@mcmaster.ca}).

O. O. Oyerinde is with the School of Electrical and Information Engineering, University of the Witwatersrand, Johannesburg, 2020, South Africa (e-mail: Olutayo.Oyerinde@wits.ac.za).

This work has been submitted to the IEEE for possible publication. Copyright may be transferred without notice, after which this version may no longer be accessible.

<b>List of Abbreviations</b>	2
<b>I Introduction</b>	2
<b>II Fundamentals of RIS</b>	4
II-A RIS Fundamentals . . . . .	4
II-B Diagonal-RIS (D-RIS) . . . . .	5
II-B1 D-RIS Architecture and Design	5
II-B2 D-RIS Modeling . . . . .	5
II-B3 D-RIS Limitations . . . . .	5
II-C Beyond diagonal RIS (BD-RIS) . . . . .	5
II-C1 BD-RIS Architecture and Design . . . . .	6
II-C2 BD-RIS Modeling . . . . .	6
II-C3 BD-RIS Merits . . . . .	6
<b>III Classification of BD-RIS</b>	7
III-A Layer 1: Based on the Scattering Matrix Type . . . . .	7
III-A1 Block Diagonal Matrix . . . . .	7
III-A2 Permuted Block Diagonal Matrix . . . . .	7
III-A3 Non-diagonal Matrix . . . . .	7
III-B Layer 2: Based on the Transmission Mode	7
III-B1 Reflective Mode . . . . .	7
III-B2 Transmissive Mode . . . . .	7
III-B3 Hybrid Mode . . . . .	8
III-B4 Multi-Sector Mode . . . . .	8
III-C Layer 3: Based on the Inter-Cell Architecture and Circuit Topology . . . . .	11
III-C1 Inter-Cell Architecture . . . . .	11
III-C2 Circuit Topology . . . . .	11
III-D Lessons Learnt . . . . .	12
<b>IV Potential Areas of Applications of BD-RIS</b>	13
IV-A Coverage Extension . . . . .	13
IV-B Physical Layer Security . . . . .	13
IV-C Multi-Cell Interference Cancellation . . . . .	13
IV-D Sensing and Localization . . . . .	14
IV-E Channel Manipulation . . . . .	14
IV-F Stacked Intelligent Metasurface (SIM) . . . . .	14
IV-G STAR-RIS . . . . .	15
IV-H Lessons Learnt . . . . .	15

<b>V</b>	<b>BD-RIS-Based Wireless Communications</b>	16
V-A	BD-RIS Architectural Development . .	16
V-B	BD-RIS Evaluation . . . . .	20
V-C	BD-RIS Integration with Emerging Technologies/Schemes . . . . .	20
V-C1	mmWave/THz Communications . . . . .	20
V-C2	ISAC Systems . . . . .	21
V-C3	UAV Communications . . . . .	21
V-C4	Non-Terrestrial Networks . . . . .	21
V-C5	MEC Networks . . . . .	21
V-C6	Radar Communications . . . . .	22
V-C7	SWIPT/WPT Systems . . . . .	22
V-C8	URLLC Systems . . . . .	22
V-C9	RSMA and NOMA Schemes . . . . .	22
V-C10	Wideband Systems . . . . .	23
V-C11	Large-Scale Systems . . . . .	23
V-C12	Vehicular Networks . . . . .	23
V-D	Lessons Learnt . . . . .	23
<b>VI</b>	<b>Challenges and Future Research Directions in BD-RIS</b>	24
VI-A	Challenges . . . . .	24
VI-A1	CSI Estimation Acquisitions . . . . .	24
VI-A2	Joint Consideration of Non-ideal Aspects . . . . .	24
VI-A3	Continuous, Discrete, and Quantized Phase-shift Designs . . . . .	24
VI-A4	Near-field vs. Far-field Propagation . . . . .	24
VI-A5	Modeling the Inter-Sector Interference of Multi-sector BD-RIS-based Systems . . . . .	24
VI-B	Future Research Directions . . . . .	25
VI-B1	Active vs. Passive BD-RIS Structures . . . . .	25
VI-B2	Integration with Additional Emerging Wireless Technologies . . . . .	25
VI-B3	Utilizing Advanced Signal Processing Tools to Optimize BD-RIS-based Systems . . . . .	25
VI-B4	Deploying a Transmissive BD-RIS at the Receiver . . . . .	25
VI-B5	Prototyping/Experimentation . . . . .	25
VI-B6	Development of Standards for the BD-RIS Technology . . . . .	25
<b>VII</b>	<b>Conclusion</b>	26
	<b>References</b>	26

#### LIST OF ABBREVIATIONS

<b>6G</b>	Sixth generation
<b>AF</b>	Amplify-and-forward
<b>B5G</b>	Beyond fifth-generation
<b>BD-RIS</b>	Beyond diagonal RIS
<b>BF</b>	Beamforming
<b>BS</b>	Base station

<b>CF-mMIMO</b>	Cell-free massive MIMO
<b>CNN</b>	Convolutional neural network
<b>CoMP</b>	Coordinate multi-point
<b>CRB</b>	Cramér-Rao bound
<b>CRN</b>	Cognitive radio network
<b>CSI</b>	Channel state information
<b>D-RIS</b>	Diagonal RIS
<b>D2D</b>	Device-to-Device
<b>DF</b>	Decode-and-forward
<b>DFRC</b>	Dual-function radar-communication
<b>EE</b>	Energy efficiency
<b>ER</b>	Energy receiver
<b>ETSI</b>	European telecommunications standards institute
<b>HAPS</b>	High altitude platform station
<b>IOS</b>	Intelligent omni-surface
<b>IoT</b>	Internet of things
<b>IR</b>	Information receiver
<b>ISAC</b>	Integrated sensing and communications
<b>ISG</b>	Industry specification group
<b>LEO</b>	Low earth orbit
<b>LoS</b>	Line-of-sight
<b>LS</b>	Least squares
<b>MEC</b>	Mobile edge computing
<b>MIMO</b>	Multiple-input multiple-output
<b>MISO</b>	Multiple-input single-output
<b>ML</b>	Machine learning
<b>mMIMO</b>	Massive MIMO
<b>mmWave</b>	Millimeter wave
<b>NLoS</b>	Non-line-of-sight
<b>NOMA</b>	Non-orthogonal multiple access
<b>NTN</b>	Non-terrestrial networks
<b>OFDMA</b>	Orthogonal frequency division multiple access
<b>OMA</b>	Orthogonal multiple access
<b>OWC</b>	Optical wireless communication
<b>PLS</b>	Physical layer security
<b>QC</b>	Quantum computing
<b>QoS</b>	Quality of service
<b>RF</b>	Radio frequency
<b>RIS</b>	Reconfigurable intelligent surface
<b>RSMA</b>	Rate splitting multiple access
<b>Rx</b>	Receiver
<b>SCNR</b>	Signal-to-clutter-plus-noise ratio
<b>SDMA</b>	Space division multiple access
<b>SE</b>	Spectral efficiency
<b>SEP</b>	Symbol error probability
<b>SIM</b>	Stacked intelligent metasurface
<b>SISO</b>	Single-input single-output
<b>SNR</b>	Signal-to-noise ratio
<b>STAR-RIS</b>	Simultaneous transmitting and reflecting reconfigurable intelligent surface
<b>SWIPT</b>	Simultaneous wireless information and power transfer
<b>THz</b>	Terahertz
<b>Tx</b>	Transmitter
<b>UAV</b>	Unmanned aerial vehicle
<b>UE</b>	User equipment
<b>URLLC</b>	Ultra-reliable low-latency communication
<b>WPT</b>	Wireless power transfer

## I. INTRODUCTION

**I**N recent years massive research efforts have been directed towards reconfigurable intelligent surface (RIS) technology in both academia and industry. These efforts were motivated by the fact that the RIS is considered a revolutionary technology for beyond fifth-generation (B5G) and sixth generation (6G) wireless communications networks due to its ability to build controllable radio environments and enhance the quality of communication in a cost-effective way [1]–[3]. Metamaterials are commonly used to build the RISs [4] as a reflective array that is made up of a large number of passive elements. Each of these elements can reflect the incident signals passively using a controllable phase shift [5]. The passive nature of

the metamaterials used to build RISs that, in turn, leads to the requirement of low power consumption of the device together with its cost-effective architecture lends credence to why RISs have attracted extensive attention. To be specific, some of the advantages of RISs include [6]: (i) Simplicity of usage: Because RISs are electromagnetic-based, virtually passive devices, and inexpensive, they can be used on a variety of structures, including building facades, interior walls, aerial platforms, roadside billboards, highway polls, car windows, and pedestrian clothing [7]. (ii) Enhanced spectral efficiency and throughput: By making up for power loss over extended distances, RISs can change the wireless propagation environment. Also, by passively reflecting the incoming radio signals with the aid of RISs, base stations (BSs) and mobile users can establish virtual line-of-sight (LoS) connections. When barriers, like high-rise buildings, obstruct the LoS link between BSs and users, the throughput enhancement becomes considerable. (iii) High compatibility with existing networks' hardware: Because RISs only reflect electromagnetic waves, they are compatible with many existing communications systems. Furthermore, existing wireless networks' standards are compatible with RIS-assisted wireless communications networks [8]. (iv) Environmentally and energy friendly: RISs can shape the incoming signal by adjusting the phase shift of each reflecting element in contrast to the conventional relaying systems like amplify-and-forward (AF) and decode-and-forward (DF) [9], which control the power amplifier. As a result, using RISs instead of traditional relaying systems is more environment- and energy-friendly [10].

Generally, in terms of mode of operation, RISs can be divided into three main categories. These include reflective mode, transmissive mode, and hybrid mode [11]. In terms of its architectural design, RISs employ single-connected architecture. In single-connected architecture, each port of the RISs is directly connected to a load and then to the ground, while there are no interconnections between ports. This absence of connections between the RIS's ports results in a diagonal scattering matrix which places constraints on RISs' signal manipulation flexibility, and beamforming (BF) capabilities, as well as introduces some potential vulnerabilities, as elaborated in Section II-B. It is worth noting that because traditional RISs have diagonal scattering matrices, sometimes they are called diagonal RISs (D-RISs) [12].

To overcome the above constraints, D-RISs has been scaled up to a more robust version called beyond diagonal RISs (BD-RISs). There are various proposed BD-RIS architectures that feature interconnections between all or a subset of the BD-RIS ports. As such the scattering matrix of these architectures is not limited to being diagonal. For example, the scattering matrix becomes a full matrix in the case where each of the ports of the BD-RISs is connected to all the other ports of the BD-RISs (i.e., fully-connected BD-RIS), and satisfies the constraints of being unitary and symmetry. The unitary constraint is due to the lossless property of the system, which means that there is energy conservation because there is no loss of energy when the signal waves interact with the scattering surface. The symmetry constraint is due to the possibility of using a reciprocal impedance network to simplify the BD-

RISs circuit. As such, based on the scattering matrix being a full matrix, there is an advantage of not only being able to control the phase of each of the BD-RISs' elements, but also the amplitude, polarization, and direction of the impinging signal waves. Different structures of the BD-RISs have been put forward to operate in different transmission modes, such as reflective, transmissive, hybrid, and multi-sector modes. Also, to operate in different circuit topologies, such as fully-/group-/tree-/forest-connected. All of the aforementioned transmission modes and circuit topologies are discussed in Section III.

Consequent to the advantages associated with deploying D-RISs in wireless communications networks, several reviews on D-RISs were documented in the literature, for example, [4], [6], [11], [13], [14]. As BD-RISs can be considered as a generalization of D-RISs, there is a merit in dedicating a survey to advocate their potential. As far as the authors are aware, there is no existing comprehensive survey conducted about BD-RISs. Therefore, this survey addresses the knowledge gap by providing a comprehensive overview of BD-RIS. Specifically, it highlights BD-RIS modeling, advantages, scattering matrix types, transmission modes, inter-cell architectures, circuit topologies, potential applications, architectural developments, performance evaluation, integration with emerging wireless technologies, challenges, and promising future research directions by emphasizing on the following aspects:

- *Classification of BD-RIS*: We first provide a comprehensive study on BD-RIS, covering key aspects of their modeling, structural characteristics, and network integration. We review various BD-RIS modeling approaches based on multiport network theory, graph theory, and matrix theory, highlighting their applicability to different use cases. The enhanced capabilities of BD-RIS over D-RIS are discussed, emphasizing their potential to enable more robust and adaptable wireless networks. Furthermore, we explore the structural diversity of BD-RIS, including different scattering matrix types (block diagonal, permuted block diagonal, and non-diagonal), transmission modes (reflective, transmissive, hybrid, and multi-sector), inter-cell architectures (single-, fully-, group-, and dynamically group-connected), and circuit topologies (single-, fully-, group-, tree-, and forest-connected). By highlighting these aspects, we provide a thorough insight into BD-RIS and its transformative potential in future wireless communications networks.
- *BD-RIS Potential Applications*: We provide an in-depth investigation of the diverse potential applications of BD-RIS structures in next-generation wireless communications networks. Specifically, we explore how BD-RIS can (i) extend wireless coverage by intelligently reflecting and refracting signals to mitigate blockages and enhance connectivity in complex environments, (ii) improve physical layer security (PLS) by enabling precise control over signal propagation to suppress eavesdropping threats and improve secure transmission, (iii) facilitate multi-cell interference cancellation in dense networks by dynamically reconfiguring the wireless environment to suppress inter-cell interference and enhance spectral efficiency, (iv) improve precise sensing and localization in

integrated sensing and communications (ISAC) systems by leveraging advanced wave manipulation to achieve high-resolution target detection and positioning, (v) enable advanced channel manipulation capabilities, allowing for customized signal shaping and adaptive BF to optimize communication performance. These applications emphasize the pivotal role of BD-RIS in enhancing network efficiency, security, and reliability in future wireless systems.

- *BD-RIS Architectural Development:* First, we present the details of some new BD-RIS architectures, such as (i) the opposite link with horizontally-connected sectors BD-RIS, (ii) the full-link with horizontally-connected sectors BD-RIS, (iii) the opposite-link with horizontally-connected sectors and vertically connected elements in each sector BD-RIS, (iv) full-link with horizontally-connected sectors and vertically connected elements in each sector BD-RIS, (v) coordinated BD-RIS, (vi) group-connected BD-RIS with dynamic and static grouping strategies, (vii) distributed BD-RIS, (viii) non-reciprocal BD-RIS and (ix) Dual-polarized BD-RIS. Second, we review the research efforts that examined the BD-RIS structure in practical systems, which include the investigation efforts of BD-RIS under mutual coupling, lossy impedance interconnections between BD-RIS elements, and with discrete-value scattering matrix. Third, we provide a discussion about the channel estimation solutions that can facilitate the operation for BD-RIS-aided systems. Furthermore, We shed some light on the research efforts that evaluated the performance of BD-RIS-aided systems from (i) an optimization perspective, (ii) a performance analysis perspective, and (iii) a circuit complexity perspective.
- *BD-RIS Integration with Emerging Wireless Technologies:* We provide a detailed investigation of how BD-RIS can be integrated with diverse emerging wireless technologies, highlighting its potential across various domains. Specifically, we discuss its integration with: (i) millimeter wave (mmWave)/terahertz (THz) communications, where BD-RIS enhances the performance of high-frequency bands by improving signal propagation; (ii) ISAC, enabling the simultaneous use of BD-RIS for both communications and precise environmental sensing; (iii) mobile edge computing (MEC), where BD-RIS facilitates the offloading of computational tasks to edge servers; (iv) radar communications, where BD-RIS can be leveraged to enhance radar signal processing, improving target detection and localization while minimizing interference; (v) simultaneous wireless information and power transfer (SWIPT) systems, where BD-RIS aids in optimizing power transmission and communication, improving energy harvesting capabilities and ensuring efficient use of radio resources; (vi) ultra-reliable low-latency communication (URLLC), where BD-RIS contributes to achieving high reliability and low latency by enabling dynamic signal control; (vii) rate splitting multiple access (RSMA) and non-orthogonal multiple access (NOMA) schemes, where BD-RIS enables more efficient spectrum utilization

and improves user fairness by facilitating advanced power control and BF strategies; (viii) wideband systems, (ix) large-scale systems, and (x) vehicular networks. Through its integration with these cutting-edge technologies, BD-RIS is positioned to play a crucial role in advancing the capabilities and efficiency of future wireless communications networks.

- *BD-RIS Challenges and Future Research Directions:* We highlight the potential of BD-RIS in addressing contemporary communications challenges that are related to (i) channel state information (CSI) estimation, (ii) joint consideration of non-ideal aspects, (iii) continuous, discrete, and quantized phase-shift designs, (iv) near-field vs. far-field propagation, and (v) modeling the inter-sector interference of multi-sector BD-RIS-based systems. Furthermore, we propose several topics for future research consideration. These topics include the investigation of (i) active vs. passive BD-RIS structures, (ii) The BD-RIS integration with additional emerging wireless technologies, (iii) utilizing advanced signal processing tools to optimize BD-RIS-based systems, (iv) deploying a transmissive BD-RIS at the receiver, (v) prototyping/experimentation, and (vi) development of standards for the BD-RIS technology.

The rest of this survey is organized as follows. Section II introduces the fundamentals, architecture and design, modeling, and the main differences between D-RIS and BD-RIS. Section III presents a detailed classification of BD-RIS in terms of its scattering matrix types, modes of transmission, and circuit design. Section IV discusses the potential areas of applications of BD-RIS. Section V discusses the various technical contributions that investigated BD-RIS from (i) the architectural development perspective, (ii) performance evaluation perspective, and (iii) its integration with the emerging technologies/schemes that are expected to meet the various requirements of B5G and 6G networks. Section VI presents challenges and potential future research directions associated with BD-RIS-aided systems. Finally, we conclude this survey paper in Section VII.

## II. FUNDAMENTALS OF RIS

### A. RIS Fundamentals

RISs are advanced electromagnetic platforms capable of dynamically manipulating signal transmission through reflection, refraction, or diffraction of radio waves. This capability enables RISs to enhance signal quality for intended receivers while minimizing interference for others [4], [13], [15]. Comprising numerous cost-effective components, RISs modify wireless channels by adjusting both the amplitude and phase of incoming signals, providing an energy-efficient alternative to traditional power-intensive methods such as power amplifiers [16]. As quasi-passive devices, RISs require minimal power to maintain their reconfigurability, with more recent models incorporating active elements in hybrid passive-active RIS structures [14]. This technology presents an economically viable and sustainable solution for improving

network coverage, data rates, energy usage, and spectral efficiency, particularly in challenging environments and non-line-of-sight (NLoS) scenarios [6]. Passive RISs, constructed from electromagnetic materials, offer a cost-effective and readily deployable solution across various infrastructures [6], [17]. Through passive signal reflection, RISs contribute to the reduction of long-distance power losses for both BSs and mobile users, presenting an energy-efficient alternative to conventional relays that necessitate power amplifiers [4]. While passive RIS facilitates full-duplex transmission through signal reflection, it is subject to multiplicative fading effects. To address this limitation, active RIS was developed, incorporating amplifiers to enhance signal strength and convert multiplicative fading into additive gains, albeit at the cost of increased power consumption [18], [19]. Furthermore, hybrid passive-active RIS designs integrate active elements to facilitate more efficient CSI acquisition [20], [21]. In contrast to reflective RISs that only support communications on one side, simultaneous transmitting and reflecting reconfigurable intelligent surface (STAR-RIS) technology enables simultaneous transmission and reflection, providing full 360° coverage and expanding its range of applications [22], [23]. Given the evolving demands of 6G and future wireless networks, RIS and advanced multiple access schemes such as RSMA [24] hold significant promise in enhancing spectral efficiency, ensuring user fairness, and improving interference management.

### B. Diagonal-RIS (D-RIS)

D-RIS, often simply called RIS, represents the earliest design of the RIS technology. In this configuration, the main function is to adjust the phase of incoming electromagnetic waves [4], using passive elements that impose phase shifts on the signals. D-RIS constrains the reflection matrix to a diagonal configuration. The architecture is primarily single-connected, enabling each D-RIS element to modify the phase shift of the incoming signal independently, without inter-element connections. The primary objective of D-RIS is to achieve a balance between performance and system complexity. By focusing only on phase adjustment, D-RIS substantially reduces computational and hardware requirements, making it practical for applications that necessitate low-latency processing and energy efficiency, such as massive MIMO (mMIMO) systems, mmWave communications, space-air-ground integrated networks, and prospective 6G wireless networks [11], [25].

1) *D-RIS Architecture and Design*: The D-RIS architecture is based on a simplified hardware design featuring a diagonal reflection matrix that simplifies control circuits and associated signal processing operations [26]. Each element within a D-RIS structure incorporates a phase-shifting component capable of altering the phase of the incoming signal. Moreover, D-RIS employs less control hardware, often implemented using adjustable passive components such as varactor diodes or micro-electromechanical systems [11]. From a design perspective, D-RIS is particularly advantageous for large-scale implementations where maintaining low energy consumption and ensuring rapid adaptation to changing channel conditions

are essential. D-RIS also supports scalable deployments in distributed networks, enhancing wireless coverage in dense urban areas and challenging NLoS scenarios [27].

2) *D-RIS Modeling*: The functioning of a D-RIS can be mathematically described by a reflection matrix, represented as  $\Theta_{\text{D-RIS}} = \text{diag}(e^{j\theta_1}, e^{j\theta_2}, \dots, e^{j\theta_M})$ , where  $M$  denotes the number of reflective elements, and  $\theta_m, \forall m \in [1, 2, \dots, M]$ , indicates the phase shift applied by the  $m$ -th element. In this diagonal configuration, each  $\theta_m$  is optimized to modify the phase of the incoming signal to improve the received signal at the intended destination [15]. The diagonal constraint simplifies the optimization problem, allowing for more efficient resource allocation and faster convergence in BF algorithms. The received signal at a user terminal can be expressed as the product of the incident signal, the channel matrix, and the diagonal reflection matrix [4]. D-RIS-based optimization aims to determine the optimal set of phase shifts  $\theta_m$  that maximizes the received signal power or other performance metrics, such as the signal-to-noise ratio (SNR) or data rate. D-RIS simplifies the process of channel estimation and reflection coefficient design, enabling more practical implementation in wireless systems.

3) *D-RIS Limitations*: D-RIS enhances signal transmission by reflecting signals with controlled phase shifts along diagonal elements of their reflection matrix. However, their functionality is limited by several factors, as summarized below.

- *Limited Flexibility in Signal Manipulation*: In a D-RIS, each element is constrained to a diagonal reflection matrix, meaning it can only apply phase shifts to the incident signals along the diagonal. This limits the ability to comprehensively control the signal's amplitude, polarization, or direction [28]. As a result, D-RIS struggles to achieve complex signal manipulations required for advanced wireless environments.
- *Limited BF Capabilities*: D-RIS offers fundamental BF functionality, primarily reflecting signals along direct LoS paths. This leads to limited beam steering flexibility and diminished performance in complex settings, such as urban or dense environments characterized by significant multipath and NLoS components [29]. As D-RIS operates using only diagonal elements, its degrees of freedom for controlling reflected signals are inherently constrained, reducing its ability to adapt to dynamic variations in user locations or environmental conditions.
- *Potential Vulnerabilities*: Due to its constrained BF capabilities, D-RIS cannot fully exploit advanced physical layer security techniques [30]. Such limitation decreases its effectiveness in countering security threats like eavesdropping and jamming, particularly in space-air-ground networks and multi-user communications scenarios.

### C. Beyond diagonal RIS (BD-RIS)

Wireless networks in the first five generations relied on advanced transmitter/receiver designs to handle the unpredictable wireless environment. Future networks (B5G and 6G) are expected to go further by using RIS to actively manipulate the wireless environment, creating what's known as a

“smart radio environment” [4], [31]. Although D-RIS features a simple design that enhances signal strength for intended users and reduces network energy consumption, its lack of inter-element coordination limits its BF abilities, resulting in reduced performance in more complex communications environments [12]. To bridge this gap and allow for more flexible signal manipulation capabilities, BD-RIS, sometimes termed as RIS 2.0, was introduced in [32] to allow for great coordination and interaction among reconfiguring elements, though at the cost of increased circuit complexity.

1) *BD-RIS Architecture and Design*: D-RIS features a simple, single-connected architecture where each element operates independently, making D-RIS structure easy to control and implement. However, this simplicity limits its ability to manipulate the electromagnetic wavefront. In contrast, BD-RIS introduces a more complex design with group-connected or fully-connected architectures, allowing for greater inter-element interaction. This enhanced connectivity enables more precise and dynamic control of electromagnetic waves, significantly improving signal manipulation and expanding RIS technology’s potential for advanced wireless communications applications. BD-RIS is conceptualized based on the analysis of scattering parameter networks [32]. Its classification is defined by its scattering matrix types, the supported transmission modes, and its inter-cell architecture and/or circuit-topology designs. All the aforementioned classification aspects are discussed in-detail in Section III.

2) *BD-RIS Modeling*: Only a few works have delved into the BD-RIS modeling to provide a convenient way of understanding the role that BD-RIS can play in wireless networks. In this regard, three main modeling approaches were investigated in the literature, namely, (i) multiport network theory [33]–[35], (ii) graph theory [36], and (iii) matrix theory [29]. The details of these approaches are elaborated as follows:

- *Multiport Network Theory*: Modeling the communications systems using multiport network theory is not new. More than a decade ago multiple-input multiple-output (MIMO) systems were analyzed using this approach, for example in [37]. This approach involves analyzing BD-RIS based on impedance ( $Z$ -parameters), admittance ( $Y$ -parameters), and scattering ( $S$ -parameters) parameters. The  $Z$ -parameters are effective for modeling mutual coupling and impedance mismatches, making them suitable for complex systems [33]. The  $Y$ -parameters, related to the  $Z$ -parameters through matrix inversion, are advantageous for modeling systems with sparse interconnections, i.e., the BD-RIS elements are interconnected by a limited number of adjustable admittance components, such as the modeling of BD-RIS-enabled wideband systems [38], [39] and tree-/forest-connected BD-RIS architectures [36]. The  $S$ -parameters excel in high-frequency radio frequency (RF) applications, as they efficiently model wave reflections and transmissions, and are particularly useful for RISs with no mutual coupling and perfect matching. In [33], a universal framework was introduced to unite the analysis of scattering, impedance, and admittance parameters for modeling BD-RIS-aided communications systems. Additionally, detailed discus-

sions were offered therein on the most preferable parameter analyses for various use cases.

- *Graph Theory*: In this approach, the BD-RIS is represented as a graph where the vertices correspond to BD-RIS ports and the edges denote tunable impedance connections between the ports. This graph theoretical approach helps in understanding the system’s complexity and performance trade-offs. Specifically, graph theory helps characterize various architectures (e.g., fully-connected, group-connected) and provides insights into how different topologies can achieve the performance upper bound with minimized circuit complexity.
- *Matrix theory*: In this approach, BD-RIS is modeled through the decomposition of the phase-shift matrix into two components: a power divider (energy allocator) system represented by a real unitary matrix, and a phase-shift system represented by a diagonal matrix. This method, termed real-unitary decomposition, simplifies the representation of complex unitary matrices, facilitating the design and analysis of BD-RIS in systems such as single-input single-output (SISO) and multiple-input single-output (MISO). The Takagi factorization [40] plays a central role in this decomposition process, ensuring that the matrix is expressed as a product of simpler matrices that still satisfy the necessary constraints for optimal communication performance. This decomposition aids in reducing computational complexity while maintaining system efficiency, especially in large-scale deployments.
- 3) *BD-RIS Merits*: Compared to D-RIS, BD-RIS provides superior BF, improved signal control, greater flexibility, higher spectrum efficiency, better interference management, and increased resilience to environmental changes. These improved features make BD-RIS a powerful and adaptable technology for enhancing future wireless communications networks, especially for B5G and 6G networks. The key benefits of BD-RIS over D-RIS are listed as follows [12], [31], [41], [42]:
  - *Precise BF in Full-Space Coverage*: Despite the fact that D-RIS and BD-RIS are both able to offer a full  $360^\circ$  coverage (through STAR-RIS and hybrid/multi-sector BD-RIS structures, respectively), multi-sector BD-RIS structure stand out by its ability to enable precise BF through high-gain elements with narrower beamwidth on each BD-RIS sector, improving the channel gain toward all intended receivers.
  - *Advanced Interference Management*: D-RIS mitigates interference by adjusting the phase of incoming signals, while BD-RIS offers effective interference management features by leveraging advanced signal processing techniques and sophisticated structures. This results in notably lower interference compared to the D-RIS counterpart.
  - *Improved Adaptability and Flexibility*: D-RIS works well in scenarios with stable and predictable signal paths. In contrast, BD-RIS provides greater adaptability to handle dynamic signal conditions such as user movement, mobile blockages, and changing network demands. This flexibility ensures reliable performance even in highly unpredictable environments.
  - *Improved Signal Manipulation Capabilities*: Unlike D-

RIS, which can only control the diagonal elements of the phase response matrix, BD-RIS offers more flexibility by enabling manipulation of both diagonal and non-diagonal elements. Specifically, D-RIS can only manipulate the phase of the signal, while BD-RIS is also capable of manipulating the signal's amplitude, polarization, and direction. These advanced manipulation capabilities greatly enhance performance in various wireless communications scenarios, particularly in 6G networks.

A comprehensive summary of the comparison between D-RIS and BD-RIS is provided in Table I.

### III. CLASSIFICATION OF BD-RIS

BD-RIS structure can be classified in terms of its scattering matrix, modes of transmission, inter-cell architecture, and circuit topology. Specifically, its scattering matrix can be either block diagonal, permuted block diagonal, or non-diagonal. Its modes of transmission can be either reflective, transmissive, hybrid, or multi-sector. Its inter-cell architecture can be either cell-wise single-/fully-/group-/dynamically group-connected architectures. Its circuit topology can be either single-/fully-/group-/tree-/forest-connected topologies. The pictorial classification of the aforementioned BD-RIS structures is illustrated in Fig. 1 as a three-layer classification tree. All these layers are discussed next in detail.

#### A. Layer 1: Based on the Scattering Matrix Type

The scattering matrix  $\Theta$  of BD-RIS structures is beyond diagonal and, under a lossless assumption, satisfies the following two constraints (i) the unitary constraint,  $\Theta^H \Theta = \mathbf{I}$ , where  $(\cdot)^H$  is the conjugate transpose operator. This means that there is energy conservation when the impinging waves interact with the scattering surface; and (ii) symmetry/reciprocal constraint,  $\Theta = \Theta^T$ , where  $(\cdot)^T$  is the transpose operator. This constraint allows for using a reciprocal impedance network to simplify the circuit of the BD-RIS system [32]. The scattering matrix of BD-RIS structures can be either block diagonal, permuted block diagonal, or non-diagonal as explained in the following.

1) *Block Diagonal Matrix*: In this scattering matrix type, the  $M$  antennas of the BD-RIS structure are uniformly divided into  $G$  groups. As illustrated in Table II(h), group-connected BD-RIS structure, a 4-element BD-RIS structure is divided into two groups of two antenna ports each, where two antennas are paired together in each group. This BD-RIS structure leads to a scattering matrix with a block diagonal structure, for which the number of blocks corresponds to the number of groups in the structure. That is,  $\Theta$  is a block diagonal scattering matrix, with each block being unitary [31]. In the case where there is only one group as shown in Table II(g), fully-connected BD-RIS structure, each of the  $M$  antenna ports is connected to all the remaining  $M - 1$  antenna ports. This makes  $\Theta$  a one-block unitary scattering matrix.

2) *Permuted Block Diagonal Matrix*: In this scattering matrix type, the way the  $M$  antennas of the BD-RIS structure are grouped can change based on the current channel conditions. In other words, the antennas' grouping strategy is dynamic and adapted to the channel environment. This dynamic grouping

allows for more flexible beam control compared to systems with fixed groupings [31]. In this case, the resulting scattering matrix is called permuted block diagonal [46] and the whole BD-RIS structure is called dynamically group-connected, as shown in Table III(h). To create an  $M$ -element permuted block diagonal scattering matrix for the dynamically group-connected BD-RIS structure, an array of switches is needed. The locations of non-zero elements in the RIS scattering matrix define the ON/OFF state of these switches. To be more precise, if the matching element in the RIS scattering matrix is non-zero, the switches are turned ON; otherwise, they remain OFF.

3) *Non-diagonal Matrix*: In this scattering matrix type, the antenna ports of the BD-RIS structure have unique interconnections. Specifically, the signal received by one antenna is reflected off another, leading to an asymmetric non-diagonal scattering matrix [49]. This architecture allows for precise control over the direction of the reflected signal, enhancing the overall performance and efficiency of the antenna system. To put this in perspective, Table II(d) and Table IV(d) are used to illustrate the D-RIS structure with a diagonal matrix and the BD-RIS structure with a non-diagonal matrix, respectively. In Table II(d), each RIS element directly reflects the impinging signal waves after phase shift adjustment. On the other hand, in Table IV(d), the signal received by one antenna element is reflected by another antenna element after phase shift adjustment. For example, in Table IV(d), by denoting the incident signal impinging on the 1-st element as  $x_1$  and denoting the reflected signal, after phase shift modification, reflected from the 2-nd element as  $y_2$ , the relationship between  $x_1$  and  $y_2$  is given as  $y_2 = x_1 e^{j\theta_{2,1}}$ . In the non-diagonal scattering matrix  $\Theta$ , each row and each column of  $\Theta$  has exactly one non-zero element, as shown in the scattering matrices provided in Table IV.

#### B. Layer 2: Based on the Transmission Mode

The modes of transmission of BD-RIS structures can be either reflective, transmissive, hybrid, or multi-sector as explained in the following.

1) *Reflective Mode*: In this category, both the transmitter and receiver are located on the same side of the BD-RIS structure as illustrated in Table II(e). Further, all the  $M$  antenna ports are oriented in the same direction. Hence, an impinging signal wave on one side of the BD-RIS structure is reflected on the same side. For this mode of transmission, the scattering matrix  $\Theta$  satisfies the unitary and symmetry constraints [31].

2) *Transmissive Mode*: In this category, a BD-RIS is deployed at the transmitter side to reduce the extensive power consumption typical of wireless transmitters that rely on fully digital RF chains to achieve high BF gains. Specifically, BD-RIS removes the requirement for extensive RF signal processing at the transmitter, while carrying out the digital BF, by modifying the phase of incoming signals with minimal power consumption [50]. Also, at the transmitter side, the BD-RIS is placed a few wavelengths away from the active transmitter antennas (as depicted in Table III(a)) to reduce the feed blockages [50].

TABLE I  
COMPARISON BETWEEN D-RIS AND BD-RIS

Feature	Diagonal-RIS (D-RIS)	Beyond Diagonal RIS (BD-RIS)
Architecture	Reflects signals with diagonal phase shifts only	Capable of reflecting and scattering signals with non-diagonal phase shifts
Connection	Single-connected scheme	Fully-connected and group-connected schemes
Signal Control	Only controls amplitude and phase shift of the reflected signal	Provides more control over signal phase, amplitude, polarization, and waveform shaping
Complexity	Simpler hardware and signal processing	More complex due to non-diagonal scattering patterns, requiring advanced control mechanisms
Flexibility	Limited to specific reflection angles and paths	Flexible in BF, allowing multi-path reflections
Beamforming	Traditional BF with limited degrees of freedom	Enhanced BF with full control over electromagnetic wavefronts
Channel Model	Suitable for simple channel models (e.g., diagonal reflection matrix)	Requires more advanced channel models due to non-diagonal elements and complex scattering behaviors
Power Consumption	Low power consumption due to simpler design and passive reflection	High power consumption due to additional complex hardware and signal processing
SNR	Moderate improvement in SNR due to limited reflection options	Significant improvement in SNR through complex scattering and multi-path propagation
Applications	Suitable for basic signal enhancement and scenarios	Suitable for more sophisticated applications such as multi-user communications and MIMO systems
Costs	Low cost due to simple hardware components and signal processing	High cost due to complex hardware components and signal processing

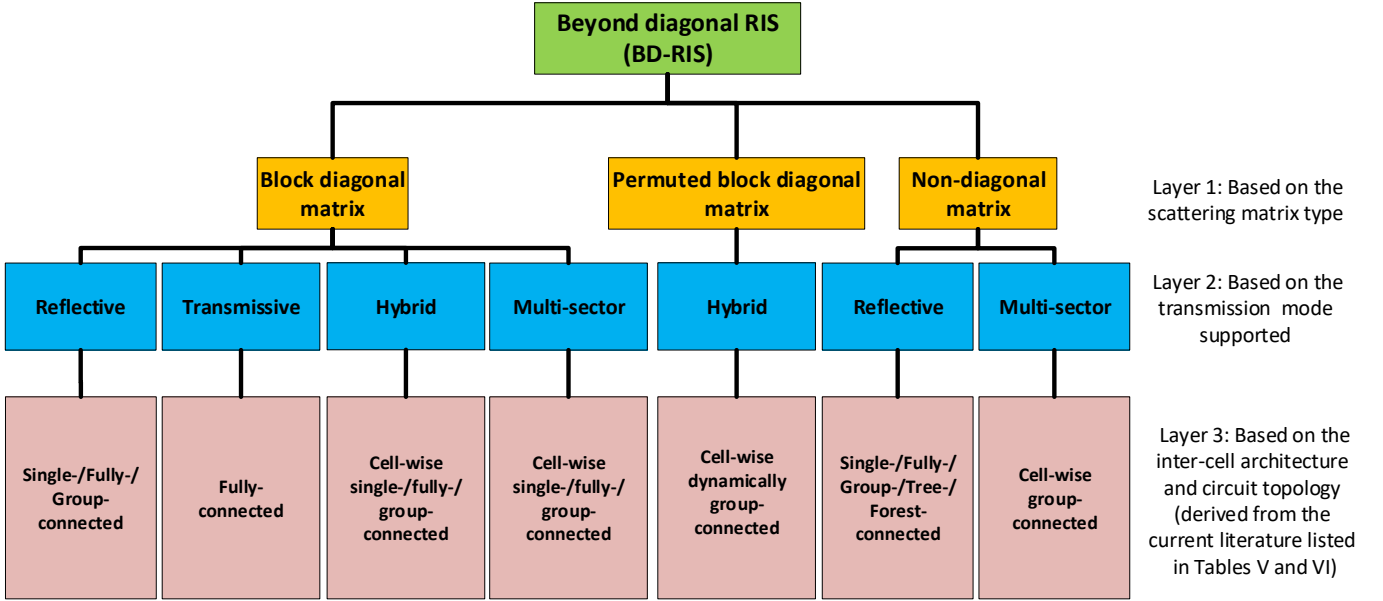


Fig. 1. BD-RIS classification tree.

3) *Hybrid Mode*: In this category, some of the impinging signal energy is reflected by the BD-RIS elements and some portion of the energy passes through to the other side of the BD-RIS structure. This mode enables coverage at the front and the back of the BD-RIS structure employing both reflective and transmissive modes, respectively, as illustrated in Table III(d). To ensure the hybrid reflective and transmissive mode, two uni-directional radiation pattern antennas are connected back-to-back to form a cell as illustrated in Table III(e)-(g). Two matrices are associated with this mode, one for the reflective mode and the other for the transmissive mode, denoted respectively as  $\Theta_r$  and  $\Theta_t$ . These two matrices satisfy the following constraint:  $\Theta_r^H \Theta_r + \Theta_t^H \Theta_t = \mathbf{I}_{\frac{M}{2}}$ , where  $\Theta_r \neq 0$  and  $\Theta_t \neq 0$  [43].

4) *Multi-Sector Mode*: In this category, the antennas are divided into multiple  $\mathcal{L} \geq 2$ -sectors, where each sector covers a limited region of space as shown in Table III(i). In this mode, when signals impinge on one sector of the BD-RIS structure, they can be partially reflected in different directions. Specifically, some of the signals may be partially reflected

towards the same sector, while others are partially scattered towards the other  $\mathcal{L}-1$  sectors. To achieve this mode, each cell is made to have  $M$  antennas that are positioned at the edges of an  $l$ -th sided BD-RIS structure. These antennas have uni-directional radiation patterns that cover  $1/\mathcal{L}$  to prevent overlap between sectors. The  $M$  antennas are connected to an  $M$ -port single-connected reconfigurable impedance network, as depicted in Table III(l) for versatile and efficient signal transmission. Consequently, the multi-sector mode can enable full-space coverage and finds applications in coverage extension in instances where there are multiple obstacles. The multi-sector mode BD-RIS has  $\mathcal{L}$ -sub-matrices,  $\Theta_l$ ,  $\forall l \in [1, 2, \dots, \mathcal{L}]$ , that satisfied the following constraint,  $\sum_{\forall l \in \mathcal{L}} \Theta_l^H \Theta_l = \mathbf{I}_{\frac{M}{\mathcal{L}}}$  [47]. In [51], the authors show that the increase in the number of sectors in the multi-sector BD-RIS, while maintaining the same total number of elements, results in substantial gains in spectral efficiency (SE) and energy efficiency (EE) compared to having fewer sectors with more elements per sector.



TABLE II  
BD-RIS CLASSIFICATION (A DETAILED LOOK)

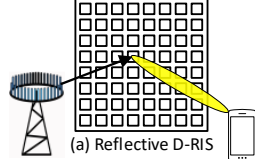
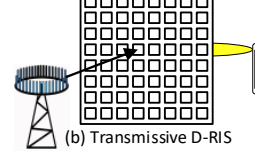
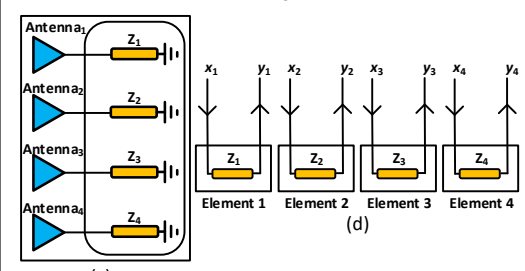
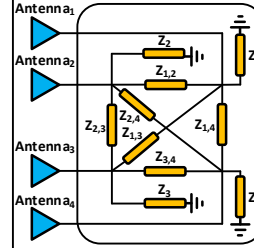
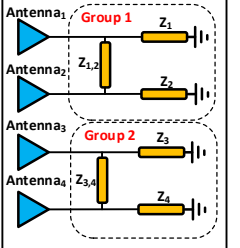
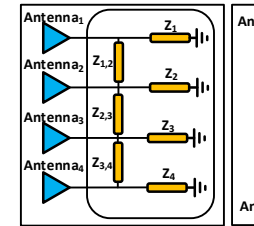
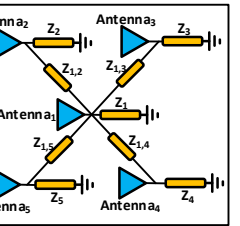
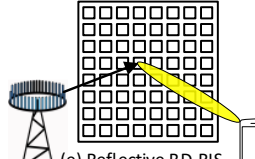
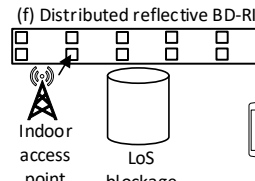
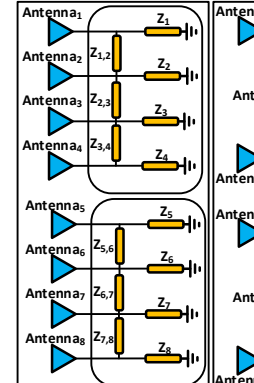
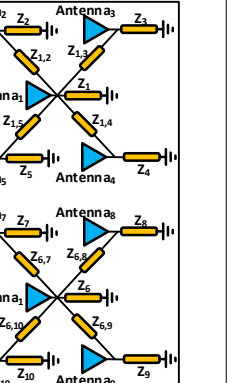
Layer 1: Scattering Matrix (With Constraints)	Layer 2: Transmission Mode (Reflective - Transmissive) D-RIS	Layer 3: Inter-Cell Architecture and Circuit Topology
<b>(Reflective - Transmissive) D-RIS</b>		
<p>→ Single-connected: [15]</p> $\Theta_{\text{D-RIS}} = \begin{bmatrix} e^{j\theta_{1,1}} & 0 & 0 & 0 \\ 0 & e^{j\theta_{2,2}} & 0 & 0 \\ 0 & 0 & e^{j\theta_{3,3}} & 0 \\ 0 & 0 & 0 & e^{j\theta_{4,4}} \end{bmatrix}$	 <p>(a) Reflective D-RIS</p>  <p>(b) Transmissive D-RIS</p>	<p>Note: In here, only reflective architecture is presented. Transmissive architecture is straightforward.</p>  <p>(c)</p>
<b>(Reflective - Distributed Reflective) BD-RIS</b>		
<p>→ Fully-connected: [43]</p> $\Theta = \begin{bmatrix} e^{j\theta_{1,1}} & e^{j\theta_{1,2}} & e^{j\theta_{1,3}} & e^{j\theta_{1,4}} \\ e^{j\theta_{2,1}} & e^{j\theta_{2,2}} & e^{j\theta_{2,3}} & e^{j\theta_{2,4}} \\ e^{j\theta_{3,1}} & e^{j\theta_{3,2}} & e^{j\theta_{3,3}} & e^{j\theta_{3,4}} \\ e^{j\theta_{4,1}} & e^{j\theta_{4,2}} & e^{j\theta_{4,3}} & e^{j\theta_{4,4}} \end{bmatrix}$ <p>Constraints: <math>\Theta = \Theta^T</math>, <math>\Theta^H \Theta = \mathbf{I}_M</math>.</p>		 <p>(g) Fully-connected</p>  <p>(h) Group-connected</p>
<p>→ Group-connected: [43]</p> $\Theta = \begin{bmatrix} e^{j\theta_{1,1}} & e^{j\theta_{1,2}} & 0 & 0 \\ e^{j\theta_{2,1}} & e^{j\theta_{2,2}} & 0 & 0 \\ 0 & 0 & e^{j\theta_{3,3}} & e^{j\theta_{3,4}} \\ 0 & 0 & e^{j\theta_{4,3}} & e^{j\theta_{4,4}} \end{bmatrix}$ <p>Constraints: <math>\Theta = \text{diag}(\Theta_1, \Theta_2, \dots, \Theta_G)</math>, <math>\Theta_g = \Theta_g^T</math>, <math>\Theta_g^H \Theta_g = \mathbf{I}_{\bar{M}}</math>, <math>\forall g, \bar{M} = \frac{M}{G}</math>.</p>		 <p>(i) Tree-connected (Tridiagonal)</p>  <p>(j) Tree-connected (Arrowhead)</p>
<p>→ Tree-connected (Tridiagonal): [36]</p> $\Theta = \begin{bmatrix} e^{j\theta_{1,1}} & e^{j\theta_{1,2}} & 0 & 0 \\ e^{j\theta_{2,1}} & e^{j\theta_{2,2}} & e^{j\theta_{2,3}} & 0 \\ 0 & e^{j\theta_{3,2}} & e^{j\theta_{3,3}} & e^{j\theta_{3,4}} \\ 0 & 0 & e^{j\theta_{4,3}} & e^{j\theta_{4,4}} \end{bmatrix}$		
<p>→ Tree-connected (Arrowhead): [36]</p> $\Theta = \begin{bmatrix} e^{j\theta_{1,1}} & e^{j\theta_{1,2}} & e^{j\theta_{1,3}} & e^{j\theta_{1,4}} & e^{j\theta_{1,5}} \\ e^{j\theta_{2,1}} & e^{j\theta_{2,2}} & 0 & 0 & 0 \\ e^{j\theta_{3,1}} & 0 & e^{j\theta_{3,3}} & 0 & 0 \\ e^{j\theta_{4,1}} & 0 & 0 & e^{j\theta_{4,4}} & 0 \\ e^{j\theta_{5,1}} & 0 & 0 & 0 & e^{j\theta_{5,5}} \end{bmatrix}$ <p>Constraints: <math>\Theta = (\mathbf{I} + jZ_0\mathbf{B})^{-1} (\mathbf{I} - jZ_0\mathbf{B})</math>, <math>\mathbf{B} = \mathbf{B}^T</math>, <math>\mathbf{B} \in \mathcal{B}_G</math>.</p>	 <p>(e) Reflective BD-RIS</p>	
<p>→ Forest-connected (Tridiagonal): [36]</p> $\Theta = \begin{bmatrix} e^{j\theta_{1,1}} & e^{j\theta_{1,2}} & 0 & 0 \\ e^{j\theta_{2,1}} & e^{j\theta_{2,2}} & e^{j\theta_{2,3}} & 0 \\ 0 & e^{j\theta_{3,2}} & e^{j\theta_{3,3}} & e^{j\theta_{3,4}} \\ 0 & 0 & e^{j\theta_{4,3}} & e^{j\theta_{4,4}} \\ e^{j\theta_{5,1}} & e^{j\theta_{5,2}} & 0 & 0 \\ e^{j\theta_{6,1}} & e^{j\theta_{6,2}} & e^{j\theta_{6,3}} & 0 \\ 0 & e^{j\theta_{7,2}} & e^{j\theta_{7,3}} & e^{j\theta_{7,4}} \\ 0 & 0 & e^{j\theta_{8,3}} & e^{j\theta_{8,4}} \end{bmatrix}$	 <p>(f) Distributed reflective BD-RIS</p>	
<p>→ Forest-connected (Arrowhead): [36]</p> $\Theta = \begin{bmatrix} e^{j\theta_{1,1}} & e^{j\theta_{1,2}} & e^{j\theta_{1,3}} & e^{j\theta_{1,4}} & e^{j\theta_{1,5}} \\ e^{j\theta_{2,1}} & e^{j\theta_{2,2}} & 0 & 0 & 0 \\ e^{j\theta_{3,1}} & 0 & e^{j\theta_{3,3}} & 0 & 0 \\ e^{j\theta_{4,1}} & 0 & 0 & e^{j\theta_{4,4}} & 0 \\ e^{j\theta_{5,1}} & 0 & 0 & 0 & e^{j\theta_{5,5}} \\ e^{j\theta_{6,1}} & e^{j\theta_{6,2}} & e^{j\theta_{6,3}} & e^{j\theta_{6,4}} & e^{j\theta_{6,5}} \\ e^{j\theta_{7,1}} & e^{j\theta_{7,2}} & 0 & 0 & 0 \\ e^{j\theta_{8,1}} & 0 & e^{j\theta_{8,3}} & 0 & 0 \\ e^{j\theta_{9,1}} & 0 & 0 & e^{j\theta_{9,4}} & 0 \\ e^{j\theta_{10,1}} & 0 & 0 & 0 & e^{j\theta_{10,5}} \end{bmatrix}$ <p>Constraints: <math>\Theta = (\mathbf{I} + jZ_0\mathbf{B})^{-1} (\mathbf{I} - jZ_0\mathbf{B})</math>, <math>\mathbf{B} = \text{diag}(\mathbf{B}_1, \dots, \mathbf{B}_G)</math>, <math>\mathbf{B}_g = \mathbf{B}_g^T</math>, <math>\mathbf{B}_g \in \mathcal{B}_{G,g}</math>, <math>\forall g</math>.</p>		 <p>(k) Forest-connected (Tridiagonal)</p>  <p>(l) Forest-connected (Arrowhead)</p>

TABLE III  
BD-RIS CLASSIFICATION (A DETAILED LOOK) (CONT.).

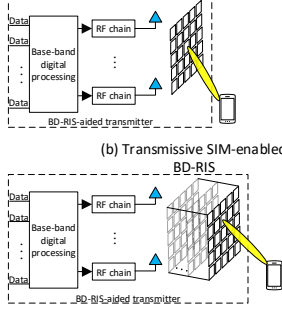
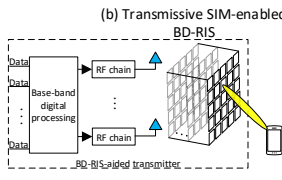
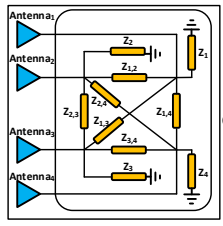
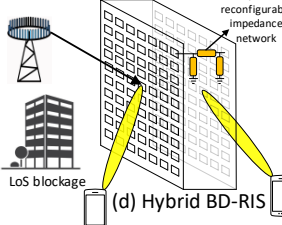
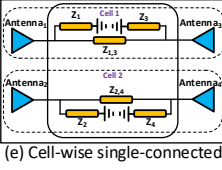
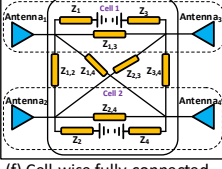
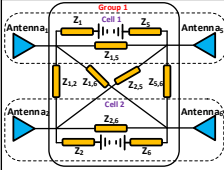
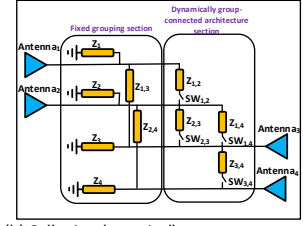
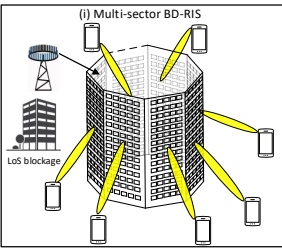
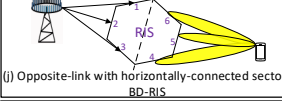
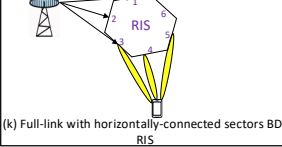
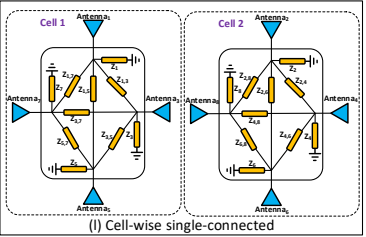
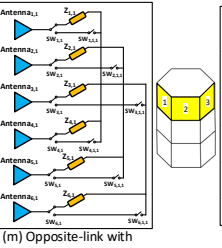
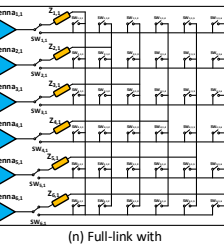
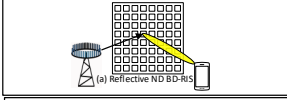
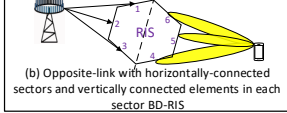
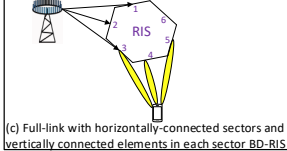
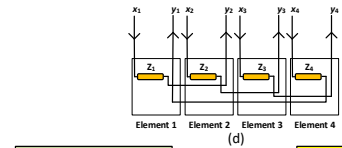
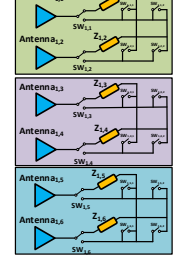
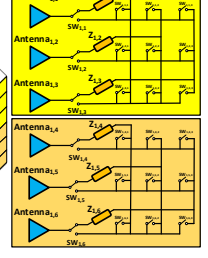
Layer 1: Scattering Matrix (With Constraints)	Layer 2: Transmission Mode (Transmissive - Hybrid - Multi-sector) BD-RIS	Layer 3: Inter-Cell Architecture and Circuit Topology
<p>→ Fully-connected: [44], [45]</p> $\Theta = \begin{bmatrix} e^{j\theta_{1,1}} & e^{j\theta_{1,2}} & e^{j\theta_{1,3}} & e^{j\theta_{1,4}} \\ e^{j\theta_{2,1}} & e^{j\theta_{2,2}} & e^{j\theta_{2,3}} & e^{j\theta_{2,4}} \\ e^{j\theta_{3,1}} & e^{j\theta_{3,2}} & e^{j\theta_{3,3}} & e^{j\theta_{3,4}} \\ e^{j\theta_{4,1}} & e^{j\theta_{4,2}} & e^{j\theta_{4,3}} & e^{j\theta_{4,4}} \end{bmatrix}$ <p>Constraints: <math>\Theta = \Theta^T</math>, <math>\Theta^H \Theta = \mathbf{I}_M</math>.</p>	<p>(a) Transmissive BD-RIS</p>  <p>(b) Transmissive SIM-enabled BD-RIS</p> 	<p>(c) Fully-connected</p> 
<p>→ Cell-wise single-connected: [43]</p> $\Theta_r = \text{diag}(e^{j\theta_{1,r}}, \dots, e^{j\theta_{M,r}}),$ $\Theta_t = \text{diag}(e^{j\theta_{1,t}}, \dots, e^{j\theta_{M,t}}),$ <p>Constraint: <math> e^{j\theta_{m,r}} ^2 +  e^{j\theta_{m,t}} ^2 = 1, \forall m \in M</math>.</p> <hr/> <p>→ Cell-wise fully-connected: [43]</p> $\Theta_r = \text{Full}(e^{j\theta_{1,r}}, \dots, e^{j\theta_{M,r}}),$ $\Theta_t = \text{Full}(e^{j\theta_{1,t}}, \dots, e^{j\theta_{M,t}}),$ <p>Constraint: <math>\Theta_r^H \Theta_r + \Theta_t^H \Theta_t = \mathbf{I}_{M/2}</math>.</p> <hr/> <p>→ Cell-wise group-connected: [43]</p> $\Theta_r = \text{blkdiag}(\Theta_{r,1}, \dots, \Theta_{r,G}),$ $\Theta_t = \text{blkdiag}(\Theta_{t,1}, \dots, \Theta_{t,G}),$ <p>Constraint: <math>\Theta_{r,g}^H \Theta_{r,g} + \Theta_{t,g}^H \Theta_{t,g} = \mathbf{I}_M, \forall g \in \mathcal{G}</math>.</p> <hr/> <p>→ Cell-wise dynamically group-connected: [46]</p> $\Theta_r = \text{blkdiag}(\Theta_{r,1}, \dots, \Theta_{r,G}),$ $\Theta_t = \text{blkdiag}(\Theta_{t,1}, \dots, \Theta_{t,G}).$ <p>Constraints: <math>[\Theta_t]_{m,n} = 0, \forall m \in \mathcal{D}_p, \forall n \in \mathcal{D}_q, p \neq q,</math>  <math>[\Theta_r]_{m,n} = 0, \forall m \in \mathcal{D}_p, \forall n \in \mathcal{D}_q, p \neq q,</math>  <math>\Theta_{t,D_g}^H \Theta_{t,D_g} + \Theta_{r,D_g}^H \Theta_{r,D_g} = \mathbf{I}_{ \mathcal{D}_g }, \forall g,</math>  <math>\mathcal{D}_p \cap \mathcal{D}_q = \emptyset, \forall p \neq q,</math>  <math>\mathcal{D}_g \neq \emptyset, \forall g,</math>  <math>\bigcup_{g=1}^G \mathcal{D}_g = M.</math></p>	<p>(d) Hybrid BD-RIS</p>  <p>(e) Cell-wise single-connected</p>  <p>(f) Cell-wise fully-connected</p>  <p>(g) Cell-wise group-connected</p>  <p>(h) Cell-wise dynamically group-connected</p> 	
<p>→ Cell-wise single-connected: [47]</p> $\Theta_l = \text{diag}(e^{j\theta_{(l-1)M+1}}, \dots, e^{j\theta_{lM}}),$ <p>Constraint: <math>\sum_{i \in \mathcal{L}_m}  e^{j\theta_i} ^2 = 1, \forall m \in M</math></p> <hr/> <p>→ Cell-wise fully-connected: [47]</p> $\Theta_l = \text{Full}(e^{j\theta_{(l-1)M+1}}, \dots, e^{j\theta_{lM}}),$ <p>Constraint: <math>\sum_{\forall l \in \mathcal{L}} \Theta_l^H \Theta_l = \mathbf{I}_{\bar{\mathcal{L}}}</math>.</p> <hr/> <p>→ Cell-wise group-connected: [47]</p> $\Theta_l = \text{blkdiag}(\Theta_{l,1}, \dots, \Theta_{l,G}),$ <p>Constraint: <math>\sum_{\forall l \in \mathcal{L}} \Theta_{l,g}^H \Theta_{l,g} = \mathbf{I}_{\bar{M}}, \forall g \in \mathcal{G},</math>  where <math>\mathcal{G} = \{1, \dots, G\}, \bar{M} = M/G</math>.</p> <hr/> <p>→ Opposite-link with horizontally-connected sectors BD-RIS: [48]  (Depending on the switch array setup, a possible <math>\Theta_l</math> can be)</p> $\Theta_l = \begin{bmatrix} 0 & 0 & 0 & e^{j\theta_{1,4}} & 0 & 0 \\ 0 & 0 & 0 & 0 & e^{j\theta_{2,5}} & 0 \\ 0 & 0 & 0 & 0 & 0 & e^{j\theta_{3,6}} \\ 0 & 0 & 0 & 0 & 0 & 0 \end{bmatrix}$ <p>Constraint: <math>\sum_{\forall l \in \mathcal{L}} \Theta_{l,g}^H \Theta_{l,g} = \mathbf{I}_{\bar{M}}, \forall g \in \mathcal{G},</math>  where <math>\mathcal{G} = \{1, \dots, G\}, \bar{M} = M/G</math>.</p> <hr/> <p>→ Full-link with horizontally-connected sectors BD-RIS: [48]  (Depending on the switch array setup, a possible <math>\Theta_l</math> can be)</p> $\Theta_l = \begin{bmatrix} 0 & 0 & e^{j\theta_{1,3}} & 0 & 0 & 0 \\ 0 & 0 & 0 & e^{j\theta_{2,4}} & 0 & 0 \\ 0 & 0 & 0 & 0 & 0 & e^{j\theta_{3,5}} \\ 0 & 0 & 0 & 0 & 0 & 0 \end{bmatrix}$ <p>Constraint: <math>\sum_{\forall l \in \mathcal{L}} \Theta_l^H \Theta_l = \mathbf{I}_M</math>.</p>	<p>(i) Multi-sector BD-RIS</p>  <p>(j) Opposite-link with horizontally-connected sectors BD-RIS</p>  <p>(k) Full-link with horizontally-connected sectors BD-RIS</p>  <p>Note: In here, only cell-wise single-connected architecture is presented. Cell-wise group/full-connected architectures are straightforward.</p> <p>(l) Cell-wise single-connected</p>  <p>(m) Opposite-link with horizontally-connected sectors BD-RIS</p>  <p>(n) Full-link with horizontally-connected sectors BD-RIS</p> 	

TABLE IV  
BD-RIS CLASSIFICATION (A DETAILED LOOK) (CONT.).

Layer 1: Scattering Matrix (With Constraints)	Layer 2: Transmission Mode	Layer 3: Inter-Cell Architecture and Circuit Topology
<b>(Reflective - Multi-sector) non-diagonal BD-RIS</b>		
<p>→ Non-diagonal (ND) BD-RIS: [49]</p> $\check{\Theta} = \begin{bmatrix} 0 & 0 & 0 & e^{j\theta_{1,4}} \\ e^{j\theta_{2,1}} & 0 & 0 & 0 \\ 0 & 0 & e^{j\theta_{3,3}} & 0 \\ 0 & e^{j\theta_{4,2}} & 0 & 0 \end{bmatrix}$ <p>Constraint: <math> e^{j\theta_m}  = 1, \forall m \in [1, 2, \dots, M]</math>.</p>		
<p>→ Opposite-link with horizontally-connected sectors and vertically connected elements: [48] (Depending on the switch array setup, a possible <math>\check{\Theta}_l</math> can be)</p> $\check{\Theta}_l = \begin{bmatrix} 0 & e^{j\theta_{1,2}} & 0 & 0 & 0 & 0 \\ e^{j\theta_{2,1}} & 0 & 0 & 0 & 0 & 0 \\ 0 & 0 & 0 & e^{j\theta_{3,4}} & 0 & 0 \\ 0 & 0 & e^{j\theta_{4,3}} & 0 & 0 & 0 \\ 0 & 0 & 0 & 0 & 0 & e^{j\theta_{5,6}} \\ 0 & 0 & 0 & 0 & e^{j\theta_{6,5}} & 0 \end{bmatrix}$ <p>Constraint: <math>\sum_{\forall l \in \mathcal{L}} \check{\Theta}_{l,g}^H \check{\Theta}_{l,g} = \mathbf{I}_{\bar{M}}, \forall g \in \mathcal{G}</math>, where <math>\mathcal{G} = \{1, \dots, G\}</math>, <math>\bar{M} = M/G</math>.</p>	 <p>(a) Reflective ND BD-RIS</p>  <p>(b) Opposite-link with horizontally-connected sectors and vertically connected elements in each sector BD-RIS</p>  <p>(c) Full-link with horizontally-connected sectors and vertically connected elements in each sector BD-RIS</p>	 <p>(d)</p>  <p>(e) Opposite-link with horizontally-connected sectors and vertically connected elements in each sector BD-RIS (Group-size = 2)</p>  <p>(f) Full-link with horizontally-connected sectors and vertically connected elements in each sector BD-RIS (Group-size = 3)</p>
<p>→ Full-link with horizontally-connected sectors and vertically connected elements in each sector BD-RIS: [48] (Depending on the switch array setup, a possible <math>\check{\Theta}_l</math> can be)</p> $\check{\Theta}_l = \begin{bmatrix} 0 & e^{j\theta_{1,2}} & 0 & 0 & 0 & 0 \\ e^{j\theta_{2,1}} & 0 & 0 & 0 & 0 & 0 \\ 0 & 0 & e^{j\theta_{3,3}} & 0 & 0 & 0 \\ 0 & 0 & 0 & 0 & e^{j\theta_{4,5}} & 0 \\ 0 & 0 & 0 & e^{j\theta_{5,4}} & 0 & 0 \\ 0 & 0 & 0 & 0 & 0 & e^{j\theta_{6,6}} \end{bmatrix}$ <p>Constraint: <math>\sum_{\forall l \in \mathcal{L}} \check{\Theta}_l^H \check{\Theta}_l = \mathbf{I}_M</math>.</p>		

### C. Layer 3: Based on the Inter-Cell Architecture and Circuit Topology

Layer 3 classification is mainly hinged on two forms. The first is the inter-cell architecture of BD-RIS structure, which is the way the cells are connected to one another in hybrid/multi-sector transmission modes. In other words, in hybrid/multi-sector transmission modes multiple uni-directionally radiating elements are arranged back-to-back to form cells [41]. The second is the circuit topology of the BD-RIS structure, which is how the antenna elements are connected to one another in reflective/transmissive modes.

1) *Inter-Cell Architecture*: In this architecture, there are cell-wise single-/fully-/group-/dynamically group-connected inter-cell architectures, as shown for the hybrid transmission mode in Table III(e)-(h). It is demonstrated in [43] that the cell-wise group-/fully-connected architecture performs better than the cell-wise single-connected architecture. In a bid to improve the performance of the cell-wise connected architecture, the inter-cell grouping technique is made adaptable to channel conditions in [46] to form what is named cell-wise dynamically group-connected architecture which is illustrated in Table III(h). The scattering matrices of this architecture can be expressed as  $\Theta_r = \text{blkdiag}(\Theta_{r,1}, \dots, \Theta_{r,G})$ ,  $\Theta_t = \text{blkdiag}(\Theta_{t,1}, \dots, \Theta_{t,G})$ , and their corresponding constraints

- are [46]
- (C1):  $[\Theta_t]_{m,n} = 0, \forall m \in \mathcal{D}_p, \forall n \in \mathcal{D}_q, p \neq q$ ,
  - (C2):  $[\Theta_r]_{m,n} = 0, \forall m \in \mathcal{D}_p, \forall n \in \mathcal{D}_q, p \neq q$ ,
  - (C3):  $\Theta_{t,D_g}^H \Theta_{t,D_g} + \Theta_{r,D_g}^H \Theta_{r,D_g} = \mathbf{I}_{|\mathcal{D}_g|}, \forall g$ ,
  - (C4):  $\mathcal{D}_p \cap \mathcal{D}_q = \emptyset, \forall p \neq q$ ,
  - (C5):  $\mathcal{D}_g \neq \emptyset, \forall g$ ,
  - (C6):  $\cup_{g=1}^G \mathcal{D}_g = M$ ,

where  $\mathcal{D} = [\mathcal{D}_1, \dots, \mathcal{D}_G]$  is an array that stores the indexes of BD-RIS cells for each group,  $(m, n)$ ,  $m \neq n$  denotes a pair of inter-connected cells connected by reconfigurable impedance components,  $\Phi_{t/r,D_g}$  is a sub-matrix of  $\Phi_{t/r}$  which selects columns and rows of  $\Phi_{t/r}$  according to indexes in the set  $\mathcal{D}_g, \forall g$ . (C1) and (C2) denote the non-zero entries in  $\Theta_t$  and  $\Theta_r$ , respectively. (C3) represents a constraint that relates  $\Theta_t$  and  $\Theta_r$  for each set  $\mathcal{D}_g, \forall g$ . (C4) ensures that every group includes a minimum of one cell. (C5) ensures that each BD-RIS cell can belong to only a single group. (C6) ensures that the different groups are mutually exclusive.

2) *Circuit Topology*: There are several proposed circuit topologies for the reflective transmission mode, namely, single-/fully-/group-/tree-/forest-connected topologies, as shown in Table III(g)-(m). If the BD-RIS structure is divided into  $G$  groups of antenna ports, while the antenna ports in each group are paired together, this refers to the group-connected topology. The scattering matrix of this topology is  $\Theta = \text{diag}(\Theta_1, \Theta_2, \dots, \Theta_G)$ , and satisfies both the unitary and symmetry constraints, which are respectively represented as  $\Theta_g = \Theta_g^T$ ,  $\Theta_g^H \Theta_g = \mathbf{I}_{\bar{M}}, \forall g$ , for  $\bar{M} = M/G$ .  $\bar{M}$  denotes the number of antenna ports in each group [32]. In

the case where there is only one group and each of the  $M$  antenna ports is connected to all the remaining  $M - 1$  antenna ports, this refers to the fully-connected topology. In single-connected topology, each element operates independently and this topology can be considered as a special case of group-connected topology [31]. The work in [32] demonstrated that the use of fully and group-connected topologies can both (i) boost the received signal power by as much as 62% compared to a single-connected architecture, (ii) achieve the same received signal power of a single-connected topology while minimizing the number of BD-RIS elements by up to 21%.

The circuit topologies for both tree-connected and forest-connected structures are modeled in [36] using graph theoretical concept and are defined as  $\mathbb{G} = (\mathbb{V}, \mathbb{E})$ , where  $\mathbb{G}$  is the graph,  $\mathbb{V}$  is the *vertex set* of  $\mathbb{G}$  and they are expressed by the set of indices of the BD-RIS ports given as  $\mathbb{V} = \{1, 2, \dots, M\}$ , and  $\mathbb{E}$  denotes the edge set of  $\mathbb{G}$ , which corresponds to the  $\bar{M}$  number of admittances connecting one port to another port in the topology. It should be noted that the number of tunable admittance components in a BD-RIS architecture's circuit topology determines its circuit complexity. Because there are  $M$  tunable admittance components connecting each element to the ground and  $\bar{M}$  tunable admittance components connecting the elements to each other, the circuit complexity of a BD-RIS represented by a graph with  $\bar{M}$  edges is therefore given by  $M + \bar{M}$ . A tree can be defined as a linked graph  $\mathbb{G}$  with  $M$  vertices and  $M - 1$  edges. Thus, a tree-connected BD-RIS has a total of  $2M - 1$  admittance components, which is significantly fewer than the  $(M(M + 1))/2$  admittance components in a fully-connected BD-RIS. This is because a tree-connected BD-RIS has  $M$  admittance components connecting each port to the ground and  $M - 1$  admittance components (edges) connecting the ports to each other. The scattering matrix of the tree-connected topology can be expressed as  $\Theta = (\mathbf{I} + jZ_0\mathbf{B})^{-1}(\mathbf{I} - jZ_0\mathbf{B})$ , where  $Z_0$  denotes the reference impedance for calculating scattering parameters and  $\mathbf{B} \in \mathcal{B}_{\mathbb{G}}$  denotes the  $M$ -port reconfigurable impedance network susceptance matrix.  $\mathcal{B}_{\mathbb{G}}$  is the set of all possible susceptance matrices for BD-RIS defined by the graph  $\mathbb{G}$  [36].

In [36], two specific examples of tree-connected topology were proposed, namely, tridiagonal and arrowhead, as illustrated in Table II(i) and (j), respectively. The tridiagonal BD-RIS structure is represented by a tree-connected topology whose graph  $\mathbb{G}$  is a path graph. On the other hand, the arrowhead BD-RIS structure is represented by a tree-connected topology whose graph  $\mathbb{G}$  is a star graph. It is worth noting that the tridiagonal BD-RIS structure is a simple and practical architecture for tree-connected topology and can be practically realized using uniform linear arrays or radio stripes. This is because it minimizes interconnection length by connecting only adjacent BD-RIS elements. However, arrowhead BD-RIS is better suited for developing tree-connected topology and can be practically realized using uniform planar arrays [36].

Forest-connected BD-RIS was proposed in [36] as a way to further minimize the circuit complexity of tree-connected BD-RIS, particularly for large-scale situations. A BD-RIS that has its  $M$  elements split up into  $\bar{M} = M/G$  groups with

group size  $G$  and uses the tree-connected architecture, i.e., each group's graph is a tree on  $G$  vertices, is known as a forest-connected BD-RIS. As a result, a forest is represented by the graph  $\mathbb{G}$  connected to the forest-connected BD-RIS. Each group in the forest-connected BD-RIS may have an arrowhead or tridiagonal tree-connected topologies [36]. Forest-connected BD-RIS, or one with  $\bar{M} = 1$ , is a special case of the tree-connected BD-RIS. Furthermore, both the single-connected and tree-connected BD-RIS are two distinct examples of the forest-connected BD-RIS, with  $G = 1$  and  $G = M$ , respectively. Furthermore, when  $G = 2$ , forest-connected BD-RIS is equivalent to a group-connected BD-RIS. In a forest-connected BD-RIS with group size  $G$ , the number of tunable admittance components is  $M((2 - 1)/G)$ . The scattering matrix of the forest-connected topology can be expressed as  $\Theta = (\mathbf{I} + jZ_0\mathbf{B})^{-1}(\mathbf{I} - jZ_0\mathbf{B})$ , where  $\mathbf{B} = \text{diag}(\mathbf{B}_1, \dots, \mathbf{B}_G)$ .

#### D. Lessons Learnt

The following points summarize the key takeaways regarding the classification of the BD-RIS architectures documented in the section.

- Due to the evolution of the RIS technology, the scattering matrix  $\Theta$  is no longer limited to being diagonal. The scattering matrix  $\Theta$  can be a block diagonal matrix where the antenna ports in each group are disconnected across groups. Further, the scattering matrix  $\Theta$  can be permuted block diagonal matrix, where grouping arrangement is adapted to the channel environment. Lastly, the scattering matrix  $\Theta$  can be an asymmetric non-diagonal scattering matrix, where the signal received by one antenna port is reflected off another antenna port.
- The operation mode of the RIS is no longer restricted to the reflective, transmissive, and hybrid transmission modes. Now the operation mode can be also multi-sector (multiple transmissive, serving multiple users located at any place around the BD-RIS structure). Full-space coverage, enhanced performance, and simplified circuit design can be achieved with the multi-sector BD-RIS-based structure in comparison with the other BD-RIS structures.
- Performance comparison between the group-connected topology and the fully-connected topology shows that as the number of BD-RIS elements increases, the SNR gain of the fully-connected topology rises quickly. However, for the group-connected topology, the larger the group sizes the higher the SNR gain, and the performance of a very large group size can approach the performance of the fully-connected topology.
- When the number of antenna ports increases significantly for the fully-connected reconfigurable impedance network, the number of reconfigurable impedance components also increases (growing quadratically with the number of antenna ports) and the circuit topology gets more complex.

#### IV. POTENTIAL AREAS OF APPLICATIONS OF BD-RIS

BD-RIS presents a promising technology in wireless communications, facilitating advancements across various domains. This section explores the potential applications of BD-RIS, which include coverage extension and enabling comprehensive signal reflection and transmission to enhance network performance in poor coverage areas. The PLS is significantly improved through the advanced BF capabilities of BD-RIS, which mitigate risks of eavesdropping and jamming. The architecture also plays a crucial role in multi-cell interference cancellation, allowing for precise signal management in dense networks. Additionally, BD-RIS enhances sensing and localization, providing accurate positioning and tracking in challenging environments. Emerging RIS types such as stacked intelligent metasurface (SIM) and STAR-RIS further expand the applications of BD-RIS, enabling innovative solutions for next-generation wireless networks. The above-mentioned applications highlight the potential of BD-RIS in addressing contemporary communications challenges.

##### A. Coverage Extension

Conventional D-RIS models are constrained to reflecting signals on a single side of the surface, resulting in limited coverage due to the uniform arrangement of antenna arrays. To address this limitation, STAR-RIS and intelligent omni-surface (IOS) were introduced in [52] and [22], respectively, enabling reflection and transmission to achieve full-space coverage. STAR-RIS, however, relies on a specific configuration with back-to-back antenna arrays and a group-connected reconfigurable impedance network [47], reducing flexibility in signal control. BD-RIS offers significant potential for enhancing network coverage. BD-RIS extends the coverage capability by enabling signal reflections and transmissions on multiple sides of the surface. BD-RIS is particularly advantageous for cellular networks, where signal degradation often limits coverage at the cell edges. By deploying BD-RIS at strategic locations, such as cell boundaries or areas with poor coverage, these surfaces can reflect and redirect signals to users outside the conventional coverage area while simultaneously enhancing the quality of service for users within the cell. Furthermore, the flexible configuration of BD-RIS allows for adaptive optimization of signal propagation paths, significantly improving network performance in dense urban, rural, or obstructed environments. In [47], the authors proposed a multi-sector BD-RIS which extends the functionality of STAR-RIS and IOS models to provide comprehensive full-space coverage. Multi-sector BD-RIS design surpasses traditional RIS and STAR-RIS performance by utilizing group-connected reconfigurable impedance networks and optimized antenna array arrangements. With its ability to deliver full-space coverage, generate highly directional beams, and adapt to varying sector configurations, the multi-sector BD-RIS is ideal for diverse applications, particularly in mmWave, THz, and cell-free network deployments.

##### B. Physical Layer Security

Conventional D-RIS provides a valuable opportunity to improve PLS in wireless communications systems by leveraging

its capability to manipulate the characteristics of the wireless channel intelligently [53]. Integrating D-RIS with advanced technologies such as Device-to-Device (D2D) communications [54], unmanned aerial vehicle (UAV) [55], internet of things (IoT) [56], and cognitive radio network (CRN) [57] highlights its flexibility in enhancing PLS. However, the limited BF capabilities of D-RIS restrict the ability to fully leverage advanced PLS techniques. Such limitation reduces its effectiveness in mitigating security threats, such as eavesdropping and jamming, especially in complex environments like multi-user communications scenarios. Consequently, D-RIS could not be suitable for applications that require robust protection against unauthorized access. On the other hand, BD-RIS offers a promising enhancement for PLS in wireless communications networks by enhancing the BF capabilities, which could significantly improve security measures by allowing for more precise control over signal propagation and maintaining robust and secure transmission. For example, by utilizing its advanced multi-sector and hybrid reflection-transmission capabilities, BD-RIS can direct confidential signals toward intended receivers while introducing artificial noise to confuse potential eavesdroppers. The architecture allows for dynamic BF across multiple sectors, enabling secure communications paths that exploit the randomness of fading channels and noise to limit unauthorized interception. Unlike conventional D-RIS, BD-RIS can flexibly manage amplitude and phase shifts, ensuring that confidential information is transmitted to legitimate users while reducing signal leakage toward eavesdroppers. Such adaptability significantly enhances PLS, particularly in complex wireless environments such as mmWave and THz networks, where secure and efficient communication is paramount.

##### C. Multi-Cell Interference Cancellation

Future cellular networks are anticipated to feature densely deployed small cells with extensive overlapping coverage areas, significantly intensifying multi-cell interference [58]. Managing and mitigating such interference is a critical challenge in dense wireless environments, and BD-RIS could be a potential solution. One of the key applications of BD-RIS is the ability to effectively reduce multi-cell interference by intelligently controlling the propagation of signals. Specifically, by leveraging a hybrid or multi-sector BD-RIS architecture, the system can be configured to manipulate the transmitted and reflected signals more precisely. The BD-RIS architecture allows for the selective nullification of signals directed toward unintended cell-edge users, minimizing the interference experienced by neighboring cells. Simultaneously, BD-RIS can enhance signal transmission by directing and reflecting signals specifically toward the intended cell-edge users, improving signal quality and overall system performance.

The advanced control mechanisms of BD-RIS, utilizing a non-diagonal scattering matrix, enable effective management of complex signal interactions across multiple sectors or cells. BD-RIS optimizes coverage, mitigates interference, and enhances spectral efficiency in densely populated cellular environments by dynamically adjusting signal transmission

and reflection characteristics. Consequently, the deployment of BD-RIS signifies a substantial advancement in tackling the challenges of multi-cell interference in the next-generation wireless communications networks. Deploying BD-RIS for passive MU BF in MU-MISO systems was explored in [28]. The design of the BD-RIS scattering matrix was utilized to either maximize the aggregate received signal power at user terminals or reduce interference at users through the zero-forcing method. A generalized practical frequency-dependent reflection model was proposed in [59] as a framework for configuring fully-connected and group-connected BD-RIS in multi-band MIMO networks. The findings highlighted potential harmful interference from insufficient synchronization between BD-RIS and adjacent BSs.

#### D. Sensing and Localization

ISAC has become a key enabler for next-generation wireless networks due to its ability to share spectrum, hardware, and signal processing between communications and sensing functions [60], [61]. The integration of mmWave technology enhances ISAC systems by offering high data rates for communications and high resolution for target sensing. However, mmWave's short wavelength leads to significant path loss, requiring numerous transmit antennas and fully digital RF chains to achieve high BF gains, which results in high power consumption [62]. Therefore, cost-effective solutions are needed for mmWave-based ISAC systems. The advanced BF capabilities of BD-RIS substantially enhance the network's ability to achieve ultra-precise device localization. These features are critical for creating a new generation of indoor positioning systems that operate independently of additional infrastructure, costs, or energy requirements [41].

The emerging BD-RIS architecture has improved BF capabilities compared to D-RIS. Using fully-connected BD-RIS to enhance throughput in ISAC systems while ensuring quality sensing was investigated in [63], demonstrating the benefits of integrating BD-RIS into ISAC networks. The authors of [64] investigated using BD-RIS to minimize the BS's transmit power in an ISAC network while ensuring communication and sensing quality. The effectiveness of the proposed system model demonstrated the advantages of BD-RIS deployment. Integrating fully connected BD-RIS into ISAC systems was investigated in [65], with its additional degrees of freedom leveraged through non-zero off-diagonal elements in the scattering matrix. By jointly optimizing the weighted sum of SNR for both radar receivers and communications users, substantial performance gains for ISAC systems were obtained. In [66], distributed BD-RIS was examined as a solution to the limited coverage of conventional and localized BD-RIS systems restricted to serving nearby users. BD-RIS elements were distributed across a wide area, and significant performance gains over both distributed D-RIS and localized BD-RIS were revealed due to the interconnections facilitating signal propagation. The BD-RIS-aided dual-function radar-communication (DFRC) system was presented in [67], differing from D-RIS-aided DFRC systems that utilized a diagonal scattering matrix, which limited signal reflection to half-space.

The BD-RIS was designed to support hybrid reflecting and transmitting modes, allowing for flexible architectures and full-space coverage, enhancing system performance and highlighting the superior communications and sensing capabilities of the BD-RIS-aided DFRC system compared to D-RIS-aided DFRC systems. A localization approach for next-generation communications systems was proposed in [68] using BS-assisted passive BF with BD-RISs. More control over phase and amplitude was obtained by BD-RISs compared to D-RISs, leading to enhanced localization accuracy. These findings highlighted the potential of BD-RISs as a promising solution for high-accuracy positioning in future wireless networks.

#### E. Channel Manipulation

Channel shaping utilizes D-RIS to modify the wireless environment, improving various aspects such as mitigating Doppler effects, enhancing MIMO channel rank, and introducing artificial channel diversity for multiple access schemes. It separates BF into two stages: channel shaping and transceiver design, offering versatile solutions for wireless applications. Channel shaping metrics fall into two categories: singular value metrics [69], which relate to performance but are sensitive to channel perturbations, and power metrics [36], which are easier to analyze but less insightful in MIMO systems.

Most works [69]–[72] have focused on a D-RIS model, limiting control to simple phase shifts without inter-element coupling. Using a passive RIS to optimize the singular values of point-to-point MIMO channels was investigated in [73], enhancing power efficiency and data rates. A BD-RIS architecture providing greater flexibility in wave manipulation compared to the D-RIS was introduced. The achievable channel singular value regions for both RIS models were analyzed. The results showed that BD-RIS significantly improved the dynamic range of singular values, leading to better channel power and higher achievable rates, particularly as the number of RIS elements and MIMO dimensions increases. The BD-RIS was investigated in [74] for their ability to create orthogonal channels in multiuser MIMO scenarios. Practical RIS implementations with passive components and constraints on their reconfigurability were proposed. Techniques for optimal channel selection without active amplification at the RIS were introduced. Efficient channel estimation and RIS configuration techniques, to be handled at the BS, were presented. The effect of channel aging due to user equipment (UE) mobility on multi-sector BD-RIS was investigated in [75]. Unlike D-RIS, BD-RIS technology provides expanded coverage. The average sum-rate maximization problem under aging conditions was addressed by jointly designing the BD-RIS matrix and transmit precoder. Numerical results revealed the impacts of channel aging on system performance.

#### F. Stacked Intelligent Metasurface (SIM)

SIM and BD-RIS represent sophisticated advances in metasurface technology that significantly enhance the ability to manipulate electromagnetic waves in wireless communications systems. These technologies extend the performance of D-RIS. SIM employs a multi-layered or stacked configuration,

enabling precise control over transmitted and reflected signals. Leveraging the interaction between multiple metasurface layers allows simultaneous manipulation of signal parameters across various spatial dimensions [76]. In contrast, BD-RIS introduces a non-diagonal scattering matrix, which provides additional degrees of freedom for signal control, enabling more dynamic transmission and reflection of electromagnetic waves. Both SIM and BD-RIS overcome the limitations of D-RIS by offering enhanced flexibility in wavefront control, improving wireless coverage, increasing signal quality, and optimizing spectral and energy efficiency [77].

The SIM achieves a non-diagonal scattering matrix involving leveraging a multi-layer RIS architecture, as proposed in [76], [78]. The SIM architecture consists of multiple closely spaced refracting metasurfaces, each designed to manipulate the incident signal progressively as it propagates through the layers [78]. Upon illumination by the incoming signal, the first metasurface layer refracts the signal toward the subsequent layer, and this process continues until the signal reaches the final layer. At this stage, the wave is radiated toward the receiver. During the propagation through the layers, the signal is dynamically shaped by tunable meta-atoms embedded in each layer, resulting in a non-diagonal end-to-end scattering matrix. This effect arises due to the inherent broadcast nature of wireless signals as they propagate from one layer to the next. A non-diagonal scattering matrix can be realized by employing dynamic refracting metasurfaces, each equipped with electronics capable of tuning the signal's phase and amplitude across layers. The scattering matrix comprehensively describes the scattering behavior of an  $M$ -port reconfigurable impedance network independent of specific circuit designs [78]. The resulting scattering matrix is diagonal in traditional RIS implementations, where each port is only connected to its respective reconfigurable impedance.

### G. STAR-RIS

The STAR-RIS or IOS offer a more versatile approach to wireless communications systems. This hybrid mode, characterized by a mathematical model that extends beyond the conventional diagonal scattering matrix, was explored in [23], [52], [79], [80]. In [52], the physical properties of IOS were detailed, along with a model capable of programmable electromagnetic responses on both sides of the surface. The study formulated an SE maximization problem for downlink communication, where the IOS was designed to enhance the SE of a multiuser system through optimal phase shift configuration. A branch-and-bound algorithm was proposed to determine the optimal phase shifts in a finite set, providing an effective solution for IOS configuration. Simulation results demonstrated significant improvements in SE and coverage, showing that IOS-assisted systems greatly expand coverage areas compared to RIS systems that rely solely on reflection.

In [79], a comprehensive hardware model for STAR-RIS was introduced, allowing for an in-depth comparison of diversity gain between STAR-RIS and conventional RIS. This analysis used channel models tailored for near-field and far-field scenarios. The work in [80] outlined four promising

techniques for independent control of transmitted and reflected signals, essential for the practical implementation of STAR-RIS. Additionally, three hardware models were presented, each quantifying the tuning capabilities of STAR-RIS with varying degrees of precision. The corresponding channel models were categorized into five groups: three for physics-based representations, one for near-field channel modeling, and one for far-field gain calculation. The benefits and limitations of these modeling techniques were thoroughly discussed. Further advancements were reported in [23], where IOS was explored for enabling full-dimensional wireless communications. Based on this concept, a hybrid BF technique was proposed for IOS-based communications systems. Additionally, a prototype of an IOS-aided wireless system was developed, with experimental results confirming the ability of IOS to simultaneously support users on both sides of the surface, demonstrating the practicality and effectiveness of the technology in real-world scenarios.

### H. Lessons Learnt

This section explores the various applications of BD-RIS. Here are the key takeaways:

- BD-RIS enhances network coverage by enabling signal reflections and transmissions from multiple sides of the surface. Such capability addresses the limitations of D-RIS models, which often struggle with LoS restrictions in urban environments. BD-RIS allows for flexible optimization of signal propagation paths, thus improving coverage in challenging areas such as dense urban landscapes and rural zones. By dynamically adapting the signal paths, BD-RIS can fill coverage gaps and ensure reliable connectivity for users in various locations.
- BD-RIS is crucial in enhancing ISAC capabilities. It enables ultra-precise localization and positioning by using reflective surfaces to interact with multiple signals and gather data from the environment. Such ability is particularly beneficial for applications in autonomous vehicles and smart cities, where accurate positioning is essential.
- BD-RIS effectively addresses multi-cell interference by intelligently controlling the propagation of signals. BD-RIS enhances spectral efficiency in densely populated cellular environments by optimizing coverage and minimizing interference between adjacent cells. The advanced control mechanisms employed by BD-RIS allow for the coordination of signals across different cells, reducing the impact of interference and improving the service quality for users in congested areas.
- BD-RIS employs channel-shaping techniques to improve various aspects of wireless communication, such as mitigating Doppler effects caused by moving objects and enhancing the rank of MIMO channels. Such channel manipulation allows for the optimization of signal transmission, increasing the reliability and efficiency of data delivery. BD-RIS's versatility in channel manipulation offers diverse solutions for applications ranging from mobile communications to IoT devices, ensuring robust performance across different scenarios.

- SIM and BD-RIS multi-layered approach provides greater flexibility in wavefront control, enabling improved wireless coverage, signal quality, and energy efficiency. SIM's ability to adjust the phase and amplitude of signals across different layers allows for optimized signal propagation and better performance in complex environments.

## V. BD-RIS-BASED WIRELESS COMMUNICATIONS

The existing technical works that investigated BD-RIS up till the time of preparing this article are discussed in this section. Tables V and VI provide a comprehensive summary of the various technical contributions that investigated BD-RIS. For ease of referencing, the headings of this section are categorized based on the "Technical content" column of Tables V and VI. Specifically, one can classify all the technical contributions that investigated BD-RIS into five main areas, namely, (i) contributions that delve into the BD-RIS modeling (Covered in Section II), (ii) contributions that explore the potential applications of BD-RIS (Covered in Section IV), (iii) contributions that develop new and/or enhance existing BD-RIS architectures (Covered in Section V-A), (ii) contributions that evaluate the performance of BD-RIS (Covered in Section V-B), and (iii) contributions that integrate BD-RIS in emerging technologies/schemes (Covered in Section V-C).

### A. BD-RIS Architectural Development

Beyond the discussion, mentioned in Section III, concerning the default BD-RIS architectures, researchers have (i) developed new BD-RIS architectures (e.g., new multi-sector BD-RIS architectures shown in Table III(j) and (k) and Table IV(b) and (c)), (ii) investigated BD-RIS with RF impairments (e.g., BD-RIS with mutual coupling and lossy interconnections), and (iii) proposed solutions to facilitate the BD-RIS operation (i.e., channel estimation-related solutions). A detailed discussion of such aspects is provided in this subsection.

When it comes to new BD-RIS architectures, several implementations were investigated by researchers to improve the performance of BD-RIS. First, the implementation of BD-RIS at the transmitter was proposed in [50] and [45], as shown in Table III(a) and (b), respectively. The use of BD-RIS at the transmitter helps alleviate the need for multiple fully digital RF chains, which are typically required for high BF gain in mmWave systems [84]. This reduction lowers both hardware complexity and power consumption of wireless transmitters.

Second, four new multi-sector BD-RIS architectures were proposed in [48] (as shown in Table III(j) and (k) and Table IV(b) and (c)). The first architecture is called "Opposite-link with horizontally-connected sectors BD-RIS" and is shown in Table III(j). In this architecture, the RIS elements from sectors opposite to each other are linked. For instance, if there are six sectors, sector 1 is connected to sector 4, sector 2 is linked to sector 5, and sector 3 is associated with sector 6. This design ensures that users can be served even when they are located in a sector opposite to the BS. The main merit of this architecture is that it simplifies the circuit while ensuring connectivity for users located in sectors not directly facing the BS. The second architecture is called

"Full-link with horizontally-connected sectors BD-RIS" and is shown in Table III(k). In this architecture, opposite to the first architecture, all sectors are connected, allowing any sector to communicate with another. This ensures that users can be served irrespective of their location within the coverage area. The merit of this architecture lies in its flexibility and higher performance as it can cover a wider range of user locations compared to the first architecture, though it comes with increased circuit complexity. The third architecture is called "Opposite-link with horizontally-connected sectors and vertically connected elements in each sector BD-RIS" and is shown in Table IV(b). Compared to the first one, this architecture introduces vertical non-diagonal connections within groups of RIS elements. This non-diagonal setup allows for more flexibility as the signal impinging on one element can be reflected from another. The merit of this architecture is that it enhances performance by leveraging intra-group flexibility while maintaining a relatively simple circuit design compared to fully connected architectures. The fourth architecture is called "Full-link with horizontally-connected sectors and vertically connected elements in each sector BD-RIS" and is shown in Table IV(c). This architecture combines the full-link approach of the second architecture with non-diagonal vertical connections within groups of RIS elements. The non-diagonal nature enables even more sophisticated signal routing, further enhancing performance. The main merit of this architecture is that it achieves nearly the same performance as fully connected architectures but with significantly reduced complexity and energy consumption. The four aforementioned multi-sector BD-RIS architectures attain a balance between performance, coverage, and circuit complexity, making them suitable for different deployment scenarios [48].

Third, a line of research has focused on optimizing the element connection pattern to improve the performance of the BD-RIS-aided systems. For instance, in [86], a coordinated BD-RIS architecture was proposed to combat channel fading, where both the configurable impedances and the element connection pattern can be optimized. The coordinated BD-RIS-aided system outperforms both single-connected and group-connected BD-RIS-aided systems in terms of power gain. Also, as the number of reflecting elements increases, its power gain reaches that of the fully-connected BD-RIS, but with a significantly smaller number of adjustable impedance settings. In [46], [87], dynamic and static grouping strategies for group-connected BD-RIS were proposed, respectively. Specifically, in [46], using an impedance-switch network that can alter the interconnections between BD-RIS groups, as illustrated in Table III(h), the best grouping strategy was obtained with high circuit complexity and control overhead. In [87], a static grouping strategy based on the channel statistics was proposed. This grouping strategy aims to enhance the achievable rate of group-connected BD-RIS without increasing the circuit complexity or requiring additional control overhead.

Fourth, some researchers have investigated distributed BD-RIS-aided systems [66], [85]. Usually, conventional BD-RIS, also referred to as "localized BD-RIS" [66], is deployed in the channel between the transmitter (Tx) and the receiver (Rx). Depending on the application, the deployment locations are



TABLE V  
SUMMARY OF EXISTING WORKS IN BD-RIS-BASED SYSTEMS

[#]	System related content			BD-RIS related content			Performance metric(s)
	Technical content	Main focus	System model	Scattering matrix type	Transmission mode	Architecture type	
[33]	BD-RIS modeling (covered in Sec. II)	Multipoint network theory BD-RIS modeling	SU-MIMO-DL	Block diagonal and non-diagonal	Reflective	Single-/Fully-/Group-/Tree-/Forest-connected	Received power
[34]		Multipoint network theory BD-RIS modeling	SU-MIMO-DL	Block diagonal	Reflective	-	-
[35]		Multipoint network theory BD-RIS modeling	SU-MIMO-DL	Block diagonal	Reflective	Group-connected	Received signal strength indicator
[36]		Graph theory BD-RIS modeling	SU-MISO-DL	Non-diagonal	Reflective	Tree/Forest-connected	Received power
[29]		Matrix theory BD-RIS modeling	SU-SISO-DL SU-MISO-DL MU-MISO-DL	Block diagonal	Hybrid	Cell-wise fully-connected	Sum-rate
[81]	BD-RIS applications (covered in Sec. IV)	Physical layer security	MU-MISO-DL	Non-diagonal	Reflective	Fully-connected	Ergodic sum-rate
[82]		Physical layer key generation	SU-SISO-DL	Non-diagonal	Reflective	Group-connected	Secret key rate
[83]		Wireless sensing	MU-SISO-DL/UL	Block diagonal	Multi-sector	Cell-wise fully-connected	CRB
[68]		Localization	SU-SISO-DL	Block diagonal	Transmissive	Fully-connected	CRLB
[28]		Interference nulling	MU-MISO-DL	Block diagonal	Reflective	Fully-connected	Sum-rate
[59]		Multi-cell	MU-MIMO-DL	Block diagonal	Reflective	Fully-/Group-connected	Received power
[45]		SIM-enabled BD-RIS	SU-SISO-DL SU-MIMO-DL	Non-diagonal	Transmissive	Fully-connected	Channel gain
[52]		STAR-RIS	SU-SISO-DL	Block diagonal	Hybrid	Cell-wise single-connected	SE
[73]		Channel shaping capability	SU-MIMO-DL	Block diagonal	Reflective	Fully-connected	Channel gain, rate
[75]		BD-RIS under channel aging effect	MU-MISO-DL	Block diagonal	Multi-sector	Cell-wise single-connected	Sum-SE
[74]	Channel orthogonalization	MU-MIMO-DL	Block diagonal	Reflective	Fully-connected	Channel gain	
[43]	BD-RIS architectural development (covered in Sec. V-A)	BD-RIS different architectures	MU-MIMO-DL	Block diagonal	Hybrid	Cell-wise group-/fully-connected	Sum-rate
[47]		Multi-sector BD-RIS structure	SU-SISO-DL MU-MISO-DL	Block diagonal	Multi-sector	Cell wise single-/group-/fully-connected	Received power, sum-rate
[84]		Transmitter side BD-RIS	MU-MIMO-DL	Block diagonal	Reflective	Fully-connected	SE
[48]		Multi-sector structures	SU-MISO-DL MU-MIMO-DL SU-SISO-DL	Block diagonal and non-diagonal	Multi-sector	Cell-wise group-connected	Achievable rate
[85]		Multi-BD-RIS	MU-MISO-DL	Block diagonal	Reflective	Fully-connected	Sum-rate
[86]		Coordinated BD-RIS	SU-MISO-DL	Non-diagonal	Reflective	Group-connected	Power gain
[46]		Dynamic grouping strategy	MU-MISO-DL	Permuted block diagonal	Hybrid	Cell-wise dynamically group-connected	Sum-rate
[87]		Static grouping strategy	SU-MISO-DL MU-MISO-DL	Block diagonal	Reflective	Group-connected	Channel gain, sum-rate
[66]		Lossy interconnections and distributed BD-RIS	SU-MIMO-DL	Block diagonal	Reflective	Single-/Fully-connected	Received power
[88]		Mutual coupling	SU-MIMO-DL	Block diagonal	Hybrid	Cell-wise group-/fully-connected	Channel gain
[89]		Mutual coupling	SU-SISO-DL	Block diagonal	Reflective	Fully-/Tree-connected	Channel gain
[90]		Non-reciprocal BD-RIS	MU-MIMO-DL/UL	Block diagonal	Reflective	Fully-/Group-connected	Rate
[91]		Non-reciprocal BD-RIS	MU-MIMO-DL/UL	Block diagonal	Reflective	Fully-/Group-connected	Sum-rate
[92]		Discrete-value scattering matrix	SU-SISO-DL SU-MIMO-DL	Block diagonal	Reflective	Fully-/Group-connected	Received power
[49]		Non-diagonal scattering matrix	SU-SISO-DL SU-MISO-DL MU-MIMO-DL	Non-diagonal	Reflective	Single-connected	Achievable rate, channel gain, OP, and BER
[93]		Dual-polarized BD-RIS	SU-SISO-DL	Block diagonal	Reflective	Single-/Fully-/Group-/Tree-connected	Received power
[94]		Q-stem connected architecture	MU-MISO-DL	Block diagonal	Reflective	Q-stem connected	Channel gain
[95]		Channel estimation	SU-MISO-DL	Block diagonal	Reflective	Group-connected	MSE
[96]		Channel estimation	SU-MIMO-DL MU-MISO-DL	Block diagonal	Reflective/ Hybrid/ Multi-sector	Group-connected and cell-wise group-connected	MSE, SE
[97]	Channel estimation	SU-MISO-DL	Block diagonal	Reflective	Group-connected	NMSE	
[98]	Channel estimation	SU-MIMO-DL	Block diagonal	Reflective	Group-connected	NMSE	
[99]	Channel estimation	MU-MIMO-DL	Block diagonal	Reflective	Fully-/Group-connected	NMSE, Sum-rate	

TABLE VI  
SUMMARY OF EXISTING WORKS IN BD-RIS-BASED SYSTEMS (CONT.)

[#]	System related content			BD-RIS related content			Performance metric(s)	
	Technical content	Main focus	System model	Scattering matrix type	Transmission mode	Architecture type		
[32]	BD-RIS evaluation (covered in Sec. V-B)	Modeling and Evaluation of BD-RIS architectures	SU-SISO-DL SU-MIMO-DL	Block diagonal	Reflective	Single-/Fully-/Group-connected	Received Power	
[100]		SE and EE maximization	MU-MIMO-DL	Block diagonal	Multi-sector	Cell-wise single-connected	SE, EE	
[51]		SE and EE maximization	MU-SISO-DL	Block diagonal	Multi-sector	Cell-wise single-connected	SE, EE	
[101]		Comprehensive performance analysis	MU-SISO-DL	Block diagonal	Multi-sector	Cell-wise single-connected	SNR, OP, SE, EE, SEP, diversity order	
[102]		A low-complexity BF design	MU-MISO-DL	Block diagonal	Reflective	Single-/Fully-/Group-connected	Channel gain, sum-rate	
[103]		BD-RIS performance complexity	SU-SISO-DL	Block diagonal and non-diagonal	Reflective	Single-/Fully-/Group-/Tree-/Forest-connected	Received power	
[104]		Closed-form global optimization	SU-SISO-DL SU-MISO-DL SU-MIMO-DL MU-MISO-DL	Block diagonal	Reflective	Fully-/Group-connected	Received power	
[105]		Power minimization and EE maximization	MU-MISO-DL	Block diagonal	Reflective	Fully-/Group-connected	Transmit power, EE, sum-rate	
[106]		Power, sum-rate, max-min rate, max-min EE optimization	MU-MISO-DL MU-MIMO-DL	Block diagonal	Reflective	Fully-/Group-/Tree-connected	Transmit power, EE, sum-rate	
[107]		SNR maximization	SU-SISO-DL SU-MISO-DL SU-SIMO-UL MU-SISO-UL	Block diagonal	Reflective	Fully-/Group-connected	SNR, sum-rate	
[108]		Rate maximization	SU-MIMO-DL	Block diagonal	Reflective	Fully-connected	Rate	
[109]		Capacity maximization	SU-MIMO-DL	Block diagonal	Reflective	Fully-connected	Capacity	
[110]		Sum-rate maximization	MU-MISO-DL	Block diagonal	Reflective	Fully-connected	Sum-rate	
[111]		Weighted sum-rate maximization	MU-MISO-DL	Block diagonal	Reflective	Fully-connected	Weighted sum-rate	
[112]		Max-min rate	MU-MISO-DL	Block diagonal	Reflective	Fully-connected	Max-min rate	
[113]		Max-min EE	MU-MISO-DL	Block diagonal	Reflective	Fully-connected	Max-min EE	
[114]		BD-RIS integration with emerging technologies/schemes (covered in Sec. V-C)	mmWave	MU-MIMO-DL	Non-diagonal	Reflective	Fully-connected	Worst-case user-rate
[115]			mmWave	MU-MISO-DL	Non-diagonal	Reflective	Fully-connected	SE
[116]			THz	SU-MISO-DL	Block diagonal	Reflective	Fully-connected	SE
[117]			THz	MU-MISO-DL	Block diagonal	Hybrid	Fully-connected	Rate
[50]	ISAC		MU-MISO-DL	Block diagonal	Transmissive	Fully-connected	Sum-rate, CRB	
[63]	ISAC		MU-MISO-DL	Block diagonal	Reflective	Fully-connected	Throughput	
[64]	ISAC		MU-MISO-DL	Block diagonal	Reflective	Fully-connected	Transmit power	
[65]	ISAC		MU-MISO-DL	Block diagonal	Reflective	Fully-connected	SNR	
[118]	UAV		MU-MISO-DL	Block diagonal	Reflective	Fully-connected	Sum-rate	
[12]	UAV		MU-MISO-DL	Block diagonal	Transmissive	Fully-connected	SE	
[44]	NTN		MU-SISO-DL	Block diagonal	Transmissive	Fully-connected	SE	
[119]	MEC		MU-SIMO-UL	Block diagonal	Reflective	Fully-/Group-connected	Latency, rate	
[67]	Radar		MU-MISO-DL/UL	Block diagonal	Hybrid	Cell-wise group-/fully-connected	SCNR	
[120]	Radar		MU-MISO-DL/UL	Block diagonal	Hybrid	Cell-wise single-/group-/fully-connected	Weighted sum-rate	
[121]	SWIPT		MU-MISO-DL	Block diagonal	Reflective	Fully-connected	Ergodic SE, harvested energy	
[122]	WPT		SU-SISO-DL	Block diagonal	Reflective	Fully-connected	Harvested power	
[123]	URLLC		MU-MISO-DL	Block diagonal	Reflective	Group-connected	Rate, EE	
[112]	URLLC		MU-MISO-DL	Block diagonal	Reflective	Fully-connected	Max-min rate	
[124]	RSMA integration		MU-MISO-DL	Block diagonal	Reflective	Fully-/Group-connected	Sum-rate	
[125]	RSMA integration		MU-MISO-DL	Block diagonal	Multi-sector	Cell-wise single-connected	Sum-rate	
[126]	RSMA integration	MU-SIMO-UL	Block diagonal	Reflective	Group-connected	Sum-rate		
[127]	NOMA integration	MU-MISO-DL SU-SISO-DL	Block diagonal	Reflective	Fully-/Group-connected	Sum-rate, asymptotic SNR		
[128]	Wideband system	SU-SISO-DL	Block diagonal	Reflective	Fully-connected	Capacity		
[38]	Wideband system	SU-SISO-DL	Block diagonal	Reflective	Group-connected	Average rate		
[39]	Wideband system	SU-SISO-DL	Block diagonal and non-diagonal	Reflective	Group-/Forest-connected	Average rate		
[100]	Wideband system	MU-MIMO-DL	Block diagonal	Multi-sector	Cell-wise single-connected	SE, EE		
[110]	Wideband system	MU-MISO-DL	Block diagonal	Reflective	Fully-connected	Sum-rate		
[129]	Large-scale systems	MU-MISO-DL	Block diagonal	Reflective	Fully-connected	Sum-rate		
[130]	Vehicular networks	MU-SISO-DL	Block diagonal	Reflective	Fully-/Group-connected	Sum-rate		

either closer to the Tx, in the middle between the Tx and the Rx, or closer to the Rx. On the contrary, distributed BD-RIS has two main implementations, either (i) several BD-RISs are deployed at different locations between the Tx and the Rx or (ii) a long BD-RIS is utilized, which cover all the distance between the Tx and the Rx, with a spacing between elements that can be much longer than the wavelength (See Table II(f)). Deploying multiple BD-RISs between Tx and Rx can provide several benefits in terms of coverage, channel quality, capacity, energy efficiency, security, and flexibility [85]. The distributed BD-RIS offers also several benefits over the localized BD-RIS by providing superior performance, particularly through its ability to guide electromagnetic signals within the BD-RIS circuit, resulting in higher signal gains and better coverage, especially in highly obstructed environments [66].

Fifth, BD-RIS enables advanced inter-element connections that produce non-diagonal scattering matrices, facilitating sophisticated signal control. A reciprocal BD-RIS features symmetric matrices where the surface behavior remains consistent regardless of the signal's direction of incidence. This limits its ability to simultaneously optimize different communications paths, making it effective only when uplink and downlink users are aligned or share similar channel conditions. On the other hand, non-reciprocal BD-RIS introduces an asymmetry in the scattering matrix, allowing the surface to respond differently depending on the direction of incoming waves. This unique property enables more flexible and effective handling of full-duplex scenarios where uplink and downlink users are in distinct locations, allowing both to communicate optimally with the same base station. In [90], the authors highlighted that the non-reciprocal BD-RIS achieves significant performance gains in full-duplex scenarios by overcoming the constraints of symmetric reciprocity, which reciprocal BD-RIS cannot address unless specific user alignments are met. However, these advantages come with challenges, such as complex circuit designs (to support non-reciprocity) and the need to account for structural scattering effects (that can impact the signal performance). Through theoretical analysis and simulations, this work demonstrated the superior adaptability of non-reciprocal BD-RIS, showcasing its potential for enhancing channel gains and expanding communications coverage in full-duplex systems. Later, the work in [90] was extended and generalized by [91] while focusing on sum-rate maximization perspective of non-reciprocal BD-RIS full-duplex communications.

Sixth, the authors of [93] explored the dual-polarized BD-RIS-aided systems compared to the literature that primarily analyzed BD-RIS-aided uni-polarized systems. Modern MIMO wireless systems employ dual-polarized antenna arrays to maximize the number of antennas in constrained spaces and enhance diversity by leveraging the polarization dimension [131]. In [93], the authors studied the scenarios where the Tx-Rx pair has the same polarization or an opposite polarization and assumed that half of the BD-RIS elements have vertical polarizations and the other half have horizontal polarizations. It is concluded that the BD-RIS architecture always provides a better gain than the D-RIS counterpart regardless of whether or not the Tx-Rx pair has the same

polarization or opposite polarization.

Seventh, in [94], a new circuit topology for BD-RIS structures that strikes a favorable complexity-performance trade-off in multi-user systems was proposed and named 'Q-stem connected' topology. This new topology attains the performance of the fully connected topology with a reduced circuit complexity. Also, Q-stem connected topology is a general BD-RIS topology, which can be reduced to fully connected BD-RIS, tree connected BD-RIS, and single connected RIS by adjusting the parameter 'Q'.

To ensure the reliable operation of BD-RIS in practical systems, researchers have investigated the performance of BD-RIS under RF impairments (i.e., under mutual coupling [88], [89] and lossy impedance interconnections [66] between RIS elements) and with discrete-value scattering matrix. Mutual coupling refers to the phenomenon where the electromagnetic field of one RIS element influences the electromagnetic field of another RIS element. Subsequently, the mutual coupling depends on the distances between the RIS elements. Specifically, the smaller the inter-element distance, the higher the effect of the mutual coupling. Mutual coupling can have both positive and negative effects on the overall performance of BD-RIS-aided systems. On the positive side, small spacing between the individual reflecting elements allows for packing a large number of elements in BD-RIS structure, potentially resulting in enhanced BF capabilities. However, accounting for mutual coupling can significantly increase the computational complexity of system design [88], [89]. The lossy impedance interconnections refer to the electrical connections between the individual RIS elements that introduce energy loss. This loss can be due to factors such as resistance, inductance, or capacitance within the interconnection network. Considering the effect of lossy interconnections can lead to a more realistic and practical model for BD-RIS systems. The lossy interconnections introduce additional challenges in designing and optimizing the RIS, as they can reduce the overall efficiency and limit the achievable BF performance [66]. In [92], a challenge of practical implementation where the impedance matrix values must be discretized, rather than treated as continuous, was investigated. Two primary solutions were proposed to achieve this, namely, scalar-discrete RISs and vector-discrete RISs. The scalar-discrete RIS solution discretizes each entry of the RIS impedance matrix independently, using an offline-designed codebook to minimize distortion from the discretization process. While this method is simple and has low optimization complexity, it requires more resolution bits to approach the performance of continuous-value RISs. On the other hand, the vector-discrete RIS solution jointly discretizes groups of impedance matrix entries, resulting in higher performance with fewer resolution bits, but at the cost of increased computational complexity.

To facilitate the operation of BD-RIS, several researchers have proposed channel estimation solutions for BD-RIS-aided systems [95]–[99]. In [95], a least squares (LS)-based channel estimation method was proposed for a MISO system with a single-antenna receiver assisted by a group-connected BD-RIS. The proposed LS-based channel estimation method relies solely on the variation of BD-RIS matrix. Later, the work

of [95] is extended in [96] to a multi-user MIMO system while relying also on the LS-based channel estimation method. The authors of [96] introduced a BF design based on the channel estimates and showed the channel estimation training overhead and transmission performance trade-off. In [97], novel channel estimation methods that effectively exploit the tensor structure of the received pilot signals were proposed. By formulating the combined channel as a Tucker tensor decomposition, the proposed methods decouple the estimation of individual channel matrices, leading to accurate CSI acquisition with minimal training overhead. The first solution provides a closed-form solution by solving parallel rank-one matrix approximation problems. The second solution employs an iterative estimation procedure to estimate the individual channels directly. Both methods significantly outperform conventional LS estimation while requiring significantly less training data, demonstrating the advantages of leveraging the tensor signal structure for channel estimation in BD-RIS systems. In [98], the authors proposed a decoupled channel estimation method that first utilized the LS estimate of the combined BD-RIS channel from the method in [96], and the individual BD-RIS channels are revealed by exploiting the Kronecker decomposition structure of the combined BD-RIS channel and some rank-one matrix approximation. In [99], joint channel estimation and prediction strategies for BD-RIS-aided MIMO system with both channel aging and correlated fast-fading environments were proposed. To decompose the BD-RIS cascaded channels into effective channels of reduced dimension, a Tucker2 decomposition with bilinear alternative LS was utilized. With the aid of convolutional neural network (CNN) and an autoregressive predictor, a channel prediction framework was advised. Then, a sum-rate maximization problem that optimizes the BD-RIS phase shifts while utilizing the estimated/predicted CSI was formulated and solved. The authors demonstrated through simulations the robustness of the proposed approach to channel aging with low pilot overhead and high estimation accuracy.

### B. BD-RIS Evaluation

The researchers evaluated the performance of BD-RIS from different perspectives, namely, from (i) an optimization perspective, (ii) a performance analysis perspective, and (iii) a circuit complexity perspective. A detailed discussion of such aspects is provided in this subsection.

In the literature, the performance of BD-RIS was optimized under different performance metrics, namely, the SNR maximization [107], the rate maximization [108], the capacity maximization [109], the sum-rate maximization [102], [106], [110], the weighted sum-rate maximization [111], the SE and EE maximization [51], [100], the power minimization and EE maximization [105], [106], the max-min rate [106], [112], and the max-min EE [106], [113]. For almost all these metrics and under various setups, there is consensus that the performance of BD-RIS outperforms the performance of D-RIS at the expense of high circuit complexity. Conversely, in [113], the authors found an exception to this rule for the minimum EE metric for large BD-RIS architectures. Specifically, at a certain point, the static power consumption of the circuitry in

large BD-RIS architectures overshadow the improvement in the rate performance compared to D-RIS architecture, making the BD-RIS architecture energy inefficient from the point-of-view of the EE metric. Therefore, this is an important design factor that the researchers need to pay attention to while utilizing BD-RIS architectures. In another optimization track, the work presented in [104] focused on developing closed-form global optimal solutions for the scattering matrix of the group- and fully-connected architectures. Also, [104] derived tight performance upper bounds for single-user MIMO and multi-user MISO fully-connected BD-RIS systems with negligible direct links.

A comprehensive performance analysis for the multi-sector BD-RIS was conducted in [101]. This work explores a multi-user communications system with BD-RIS operating in time-switching mode, analyzing critical metrics such as the outage probability, SE, EE, and symbol error probability (SEP). The study derives closed-form expressions for the SNR distributions and demonstrates that increasing the number of sectors within a BD-RIS significantly enhances performance, particularly in terms of the SE and the EE. However, this sectorization leads to a trade-off, improving performance but reducing diversity order. The results show substantial gains of up to 182% for the SE and up to 238% for the EE when increasing the number of sectors from 2 to 6, highlighting the benefits of sectorization while also considering the complexity and hardware requirements involved in real-world deployments.

A Pareto frontier for the trade-off between performance and complexity in different BD-RIS architectures was derived and characterized in [103]. This work aimed to determine the BD-RIS architectures that are most suited for bridging the gap between single-connected RIS and tree-connected BD-RIS.

### C. BD-RIS Integration with Emerging Technologies/Schemes

BD-RIS-assisted communications has emerged as a promising technology for improving the performance of wireless communications systems. Integrating BD-RIS technology into wireless systems offers significant potential to support robust, reliable, and long-range data transmission, helping meet the requirements of 5G and 6G wireless networks. This subsection outlines the integration of BD-RIS with a range of emerging wireless technologies and schemes, namely, mmWave/THz communications [132], [133], ISAC [62], MEC [134], radar communications [135], SWIPT systems [136], URLLC [137], the RSMA and NOMA schemes [138], [139], wideband systems [140], and large-scale systems [141].

1) *mmWave/THz Communications*: The integration of BD-RIS in mmWave/THz communications were explored in [114]–[117]. In [114], a max-min fairness optimization problem was investigated for BD-RIS-assisted mmWave MIMO system while assuming a hybrid BF at both the BS and the users and a passive BF at the BD-RIS structure. The obtained results demonstrated that, when deploying a large BD-RIS structure, the proposed system outperforms the D-RIS counterpart, in terms of the worst-case UE rate, and approaches the performance of a half-duplex relay counterpart. Also, the EE performance of the proposed system outperforms

both the D-RIS and half-duplex relay counterparts as well as the full-duplex relay counterpart at high SNR. In [115], a SE maximization problem was investigated for BD-RIS-assisted mmWave MISO system while considering both the BS BF matrix and BD-RIS scattering matrix. The obtained results demonstrated that the SE performance of the BD-RIS structure is superior to the D-RIS structure counterpart. A similar SE maximization problem was investigated in [116] but for the THz communications. In this work, the authors utilize a low-resolution digital beamformer at the BS and a discrete phase-shift design at the BD-RIS. In THz communications, employing the fully digital BF method at the BS is impractical, due to the need for a large number of RF chains for the operation of the massive number of antenna elements at the BS. Also, the obtained results in [116] demonstrated that the SE performance of the BD-RIS structure is superior to the D-RIS structure counterpart. In [117], a hybrid BD-RIS architecture employs a THz communications system to serve both an indoor user and an outdoor user. A sum-rate maximization problem that jointly optimizes the phase shifts in the hybrid BD-RIS architecture and the hybrid BF vectors of the BS was formulated and solved. The authors demonstrated through simulations the rate superiority of the proposed approach compared to time-division hybrid RIS, frequency-division hybrid RIS, and STAR-RIS counterparts.

2) *ISAC Systems*: The integration of BD-RIS in ISAC systems were explored in [50], [63]–[65]. The authors of [50] studied a joint optimization problem that maximizes the sum rate for the communications users and minimizes the largest eigenvalue of the Cramér-Rao bound (CRB) for the sensing targets. Simulation results showed that the BD-RIS-aided system attains a better communications and sensing performance compared to the D-RIS counterpart. In [63], the maximization problem of the networks' throughput while maintaining the sensing quality was analyzed. The provided simulation results revealed the BD-RIS-aided system superiority compared to the D-RIS counterpart. The authors of [64] considered a BS's transmit power minimization problem while maintaining both the communications and sensing quality. Simulation results illustrated that the BD-RIS-aided system can reduce the BS's transmit power by 25%-30% compared to the D-RIS counterpart. The authors of [65] optimized the weighted sum of the SNR at the communications users and the sensing target. Simulation results revealed that, while employing a BD-RIS structure, the SNR values for both communications users and the sensing target improve by several orders of magnitude compared to the D-RIS counterpart.

3) *UAV Communications*: The integration of BD-RIS in UAV communications was examined in [12], [118]. The representative work in [118] considered several UAVs transmitting signals to groups of users with LoS links and with NLoS links through a BD-RIS structure. It is assumed that each UAV transmitter is serving a unique user group using orthogonal frequency division multiple access (OFDMA) and the users within each group are served using the RSMA scheme. A sum-rate maximization problem that jointly considers UAVs BF design, BD-RIS elements allocation to groups, BD-RIS elements phase shifts, and the RSMA common-rate allocation

was investigated. Simulation results demonstrated that the sum-rate performance of the proposed BD-RIS-aided RSMA-assisted UAV system outperforms the counterpart schemes of (i) an RSMA-assisted D-RIS scheme, (ii) a power-domain NOMA-assisted D-RIS scheme, and (iii) an RSMA-assisted UAV system without the RIS technology. In [12], the authors highlighted the possible deployment locations of the BD-RIS structures in UAV-based systems. Notably, BD-RIS structures can be deployed into; (i) terrestrial fixed structures such as buildings to enhance the signal strength and coverage between UAV transmitters and their respective users, mainly in urban areas, (ii) aerial mobile units to resolve the NLoS blockages and maintain optimal communications links between the ground stations and their respective users, and (iii) a dual terrestrial-based and aerial-based configuration to achieve a robust system that can be suitable for a variety of use-cases. They also investigated an SE maximization problem for a BD-RIS mounted UAV multi-user MISO communications system. Through simulations, the authors illustrated the superiority of the investigated system in terms of SE performance compared to the D-RIS counterpart.

4) *Non-Terrestrial Networks*: The integration of BD-RIS in non-terrestrial networks (NTN) was examined in [41], [44]. In [41], the authors investigated a multi-user NOMA-enabled low earth orbit (LEO) satellite communications system while employing a BD-RIS structure to enhance the communications links between the LEO satellite and its ground users. A sum-rate maximization problem was studied while ensuring the quality of service (QoS) of the ground users. Simulation results revealed the superiority of the proposed BD-RIS-aided system compared to the D-RIS counterpart for different satellite transmit powers and different numbers of elements in the employed BD-RIS structure. In [44], a transmissive BD-RIS was mounted on an LEO satellite to aid the downlink NOMA transmission to two ground IoT devices. A SE maximization problem that optimizes both the LEO NOMA power allocation and the phase shift of the transmissive BD-RIS was formulated and solved. Through simulations, the authors demonstrated that the proposed optimized scheme outperforms the fixed NOMA power allocation counterpart in terms of the system's SE.

5) *MEC Networks*: In MEC networks, numerous users offload their duties to the MEC server due to restricted resources and short battery life, then the MEC server performs the heavy computations and sends back the results to the users to take actions. The authors of [119] developed a BD-RIS structure mounted on UAV to help the remote users in offloading their tasks to the MEC server that is mounted at the BS. A minimization problem for the utility function of task computational delay and UAV's hovering time was investigated. The optimization problem takes into account the location of the UAV, the BD-RIS phase shifts, the BS receive BF vector, the task segmentation variable, users transmission power, and the computational resources of the MEC server and users. The results demonstrated that (i) fully-connected and group-connected architectures exhibit superior worst-case rate performance compared to the single-connected architecture, (ii) the optimal BD-RIS deployment significantly enhances the

system's utility function relative to the conventional building-mounted RIS, (iii) the optimized offloading strategy achieves a 13.44% improvement in the system's utility function over the binary offloading strategy.

6) *Radar Communications*: DFRC technology emerged to enable spectrum sharing between radar and communication, as radar systems compete for the same limited resources. The integration of communications and radar operations into a single platform in DFRC systems results in increased spectrum efficiency, reduced power consumption, and lower hardware costs. As a result, it is anticipated that DFRC will be crucial to the development of new environment-aware applications [142], including smart homes, environmental monitoring, and automotive networks. The LoS connectivity between the BS and communications users/sensing targets are essential to the current designs of DFRC. Unfortunately, this led to two challenges: (i) barriers can readily obstruct the LoS link toward sensing targets or communications users; and (ii) considerable path-loss may occur in the LoS channels, particularly at high frequencies. The deployment of BD-RIS has the potential to resolve these challenges because BD-RIS not only achieves full-space coverage but also offers better BF capabilities than D-RIS.

A generic BD-RIS-assisted DFRC system was proposed in [67], comprising a hybrid BD-RIS structure, numerous users, and various sensing targets corrupted by multiple clutter sources. A maxmin radar output signal-to-clutter-plus-noise ratio (SCNR) optimization problem is formulated while considering the transmit waveform at the dual-function BS, the transmissive and reflective BF at the BD-RIS, and matched filters at the radar sensing receivers. Simulation results showed that group- and fully-connected BD-RIS structure exhibit superior radar SCNR performance compared to the STAR-RIS structure under identical communications constraints. Another BD-RIS-assisted DFRC system was proposed in [120] comprising also a hybrid BD-RIS structure, indoor and outdoor users, and multiple far-located sensing targets. This work investigated different BD-RIS structures, namely, the cell-wise single-/group-/fully connected structures. A maximization of users weighted sum-rate problem was considered while taking into account the transmit waveform at the dual-function BS and the transmissive and reflective BF at the BD-RIS. The provided simulation results illustrated that the cell-wise fully connected structure achieves a higher weighted sum-rate performance compared to the STAR-RIS structure for different numbers of RIS elements and BS transmit powers.

7) *SWIPT/WPT Systems*: In energy-constrained IoT networks, SWIPT presents a viable method for cost-effective power delivery [143]. A BS with a continuous power supply simultaneously broadcasts wireless signals to information receivers (IRs) and energy receivers (ERs). The main difficulty with SWIPT systems is that different power supplies are needed for the ERs and IRs to function. ERs explicitly demand received power at a far higher order than IRs. Because of the signal attenuation, the ERs' practical operating range is limited. Hence to harvest enough power, they need to be deployed closer to the BS than IRs. The operational range of ERs can be increased by deploying a BD-RIS structure

between the BS and the ERs. In [121], a BD-RIS-aided cell-free massive MIMO (CF-mMIMO) SWIPT system was proposed. An analytical framework that focuses on the ergodic SE of the IRs and the average harvested energy of the ERs was advised. The conducted simulation results illustrated the superiority of the designed BD-RIS-aided system compared to systems (i) with a random BD-RIS design and (ii) without BD-RIS structure. In [122], a multi-carrier SISO wireless power transfer (WPT) system that employed a fully-connected BD-RIS structure was proposed to mitigate the low end-to-end power transfer efficiency challenge. A receiver harvested power maximization problem that optimizes both the BS BF and the multi-carrier waveforms was formulated and solved. The authors revealed through simulations that the BD-RIS-aided system achieved the same receiver harvested power performance as the D-RIS-aided system under far-field LoS conditions, while it outperforms D-RIS-aided system under Rician pure NLoS conditions.

8) *URLLC Systems*: The integration of BD-RIS in URLLC systems was inspected in [112], [123]. In [123], the role of BD-RIS and RSMA in a MISO multi-cell URLLC system was studied. This work demonstrates that the impact of BD-RIS on the RSMA scheme varied with network load. Specifically, BD-RIS can amplify the gains of the RSMA scheme in overloaded regimes, whereas the benefits of the RSMA scheme can be attenuated or even nullified by BD-RIS optimization in underloaded regimes. Also, this work investigated the influence of packet length on the RSMA scheme performance. Specifically, the performance gains of the RSMA scheme are enhanced as packet lengths decrease or as the maximum tolerable decoding failure probability diminishes. Moreover, the combination of the RSMA scheme and the group-connected BD-RIS structure (group size 2) in URLLC systems can substantially improve the SE and the EE of the system.

In [112], the authors compared the performance of three RIS architectures, namely, locally passive D-RIS, globally passive D-RIS, and globally passive BD-RIS, in a multi-user MISO URLLC system. In locally passive D-RIS architecture, i.e., conventional D-RIS architecture, the D-RIS reflection constraints are imposed independently on each individual reflecting element, while in globally passive D-RIS/BD-RIS architectures, the D-RIS is defined by a unified reflection constraint that simultaneously affects all reflecting elements. This expanded the set of possible reflection matrices, which led to a better performance at the expense of a higher computational complexity [16]. This work solved an average max-min rate optimization problem and its findings demonstrated that the max-min rate performance of globally passive BD-RIS architecture outperforms (i) globally passive D-RIS, (ii) locally passive D-RIS, (iii) an un-optimized D-RIS, i.e., random D-RIS, and (iv) No D-RIS architectures.

9) *RSMA and NOMA Schemes*: The integration of BD-RIS with the RSMA scheme was investigated in [124]–[126]. A fully-connected BD-RIS aided downlink multi-antenna multi-user RSMA transmission paradigm was proposed in [124]. A sum-rate maximization problem that considers both the transmit beamformer of BS and the scattering matrix of BD-RIS was investigated. Through simulations, the authors

demonstrated that the sum-rate performance of the fully-connected BD-RIS outperforms both the counterparts with the D-RIS structure and without RIS. In [125], the integration of multi-sector BD-RIS and RSMA in a multiuser-MISO communications system was considered. A stochastic average sum-rate maximization problem was formulated while jointly considering the BS transmit beamformer and the BD-RIS matrix under the imperfect CSI conditions. The simulation results exhibited an improved sum-rate performance compared to the space division multiple access (SDMA) scheme. Furthermore, the results showed that the numbers of active and passive antennas, at the BS and the BD-RIS structure, respectively, can be effectively reduced with the combination of multi-sector BD-RIS with the RSMA scheme. In [126], a BD-RIS-aided uplink RSMA system was investigated. A sum-rate optimization problem that jointly considers the BS receive beamformer, the BD-RIS scattering matrix, and the UEs transmit power was formulated and solved. Simulation results showed that the sum-rate performance of the proposed BD-RIS-aided RSMA system outperforms an RIS-aided RSMA counterpart system.

The integration of BD-RIS with the power-domain NOMA scheme was investigated in [127]. In [127], an asymptotic received SNR formula for a single-user SISO NOMA-enabled BD-RIS-aided system was derived. Also, a sum-rate maximization problem for a multi-user MISO NOMA-enabled BD-RIS-aided system was formulated and solved. Simulations results indicated that the BD-RIS offers a superior square-law SNR than D-RIS and a higher sum-rate performance than both D-RIS and traditional orthogonal multiple access (OMA)-enabled systems.

10) *Wideband Systems*: The integration of BD-RIS in wideband systems was considered in [38], [39], [100], [110], [128]. It should be noted that the modeling of the BD-RIS structure in wideband applications is investigated in two directions. In [100], [128], the authors modeled the BD-RIS structure using a frequency-independent modeling method. While in [38], [39], [110], the authors modeled the BD-RIS using a frequency-dependent modeling method. The authors of [38], [39] justified this by the fact that, in wideband applications, the scattering matrix of the BD-RIS is better modeled using a reconfigurable admittance network, where the admittance of each tunable element has different values at different frequencies. The findings of [38], [39] demonstrated that the frequency-independent model facilitates the BD-RIS design, but at the expense of causing some performance loss to the BD-RIS-aided wideband systems. Also, the importance of taking into account the frequency-dependency becomes more important when the circuit complexity of the BD-RIS increases.

11) *Large-Scale Systems*: The integration of BD-RIS with the large-scale systems was investigated in [129]. This work introduced a meta-learning-based optimization framework aimed at optimizing BD-RIS-aided large-scale wireless systems. Traditional optimization techniques are computationally impractical at large scales, so the proposed framework leverages unsupervised meta-learning to reduce complexity without needing extensive training data. Specifically, a sum-rate maximization problem that jointly takes into account the

BS transmit BF and the phase-shifts of the BD-RIS scattering matrix for a multi-user MISO system was formulated and solved using the meta-learning-based optimization framework. Through simulations, the authors illustrated the performance gains of the evaluated BD-RIS-aided system compared to the D-RIS counterpart. For example, in an extreme case, the sum-rate performance of the evaluated BD-RIS-aided system with 15 antennas at the BS outperforms a RIS-aided system with 100 antennas at the BS. This shows the potential of the BD-RIS structure in reducing the complexity and energy consumption at the wireless transmitters.

12) *Vehicular Networks*: The integration of BD-RIS with vehicular networks was studied in [130]. This study investigated a multi-cell transportation network that was aided by a BD-RIS to improve the SE of the network. Also, the authors formulated and solved a sum-rate maximization problem that optimized both the BS allocation power and the BD-RIS phase shift design in each cell. Through simulations, the authors illustrated the superiority of the proposed BD-RIS-aided transportation network in terms of sum-rate performance compared to the D-RIS, STAR-RIS, and sub-optimal optimization counterpart.

#### D. Lessons Learnt

There has been progress made in the research activities that focus on the BD-RIS-based systems. Below are some key takeaways from the reviewed literature.

- There are several architectural development investigations for BD-RIS structures. These developments start by proposing different transmission modes, such as reflective, hybrid, or multi-sector to enhance the coverage in wireless systems. They also employed different circuit topologies, such as fully-/group-/tree-/forest-connected with and without cells to expand the wave-domain processing capabilities by increasing the number of optimization variables and the possible scattering matrices. Moreover, non-diagonal BD-RIS structures that allow for precise control over the direction of the reflected signal, enhancing the overall performance and efficiency of the antenna system can be adopted. Furthermore, the location of deployment of BD-RIS structures is not limited to the channel between the Tx and Rx. BD-RIS can also be deployed at the transmitter to reduce its hardware complexity and power consumption. Additionally, distributed BD-RIS structures were proposed while either utilizing several BD-RISs between the Tx and Rx or a long BD-RIS structure to achieve several benefits in terms of coverage, channel quality, capacity, energy efficiency, security, and flexibility. Knowing which structure to adopt for different use cases is a key design factor to benefit the most from the enhanced capabilities that BD-RIS can provide.
- To increase the practicality of BD-RIS structures, researchers have investigated the performance of BD-RIS under systems with non-ideal aspects, such as mutual coupling, lossy impedance interconnections, and discretized impedance values. To fully understand the potential and

challenges of BD-RIS structures in wireless systems, there is a need for examining the BD-RIS performance under additional practical scenarios, for example, with imperfect CSI, with transceiver hardware impairments, under generalized fading models that better fit real-time experimental data.

- Compared to the D-RIS structure, the optimization of BD-RIS structures is subject to additional constraints, for example, the need for the scattering matrix of the BD-RIS to be unitary, making the solution process more complex than that of the D-RIS structure. A potential approach involves relaxing the strict unitary constraint, thereby simplifying the optimization problem. However, this relaxation can compromise performance, as the derived solution may deviate from the optimal solution of the original problem. Another approach involves employing the manifold optimization algorithm that represents all feasible solutions as a geometric shape (manifold). By doing this, the original constrained problem is converted into an unconstrained problem and subsequently can be efficiently solved through standard searching techniques with minor adjustments to account for the manifold's specific properties.
- BD-RIS structures offer significant advantages in various wireless communications networks. By introducing additional degrees of freedom in phase shift control, BD-RIS can enhance signal propagation, improve channel quality, and mitigate interference. This leads to improved spectral efficiency, energy efficiency, and link reliability. In mmWave/THz communications, BD-RIS can compensate for severe path loss and BF challenges. In ISAC systems, BD-RIS can enable reliable simultaneous sensing and communications by intelligently controlling the reflected signals. In UAV communications, BD-RIS can provide flexible and dynamic coverage, while in MEC networks, it can enhance network capacity and offloading capabilities. In radar communications, BD-RIS can improve target detection and tracking performance. In SWIPT systems, BD-RIS can enhance power transfer and information reception. In URLLC systems, it can improve reliability and latency. Wideband systems benefit from BD-RIS's ability to mitigate inter-carrier interference. In large-scale systems, BD-RIS can reduce the number of active antennas and improve energy efficiency. Overall, this synergy BD-RIS structures and the aforementioned emerging technologies/schemes leads to significant gains in terms of coverage, capacity, and spectral efficiency.

## VI. CHALLENGES AND FUTURE RESEARCH DIRECTIONS IN BD-RIS

In this section, we discuss some key challenges and future research directions of BD-RIS-aided wireless communications systems.

### A. Challenges

Despite the benefits and potential applications of BD-RIS, there exist some challenges with respect to its implementation, such as:

1) *CSI Estimation Acquisitions*: To take full advantage of the benefits provided by the BD-RIS and to ensure coherent signal detection in the BD-RIS-based wireless communications networks, there is a need for the provision of accurate CSI. The semi-passive channel estimation strategy in which D-RIS is equipped with a few low-power RF chains to enable the pilot transmission/reception for channel estimation can still be employed in some BD-RIS-based systems. However, this will be at the expense of additional power consumption due to the introduced RF chains. Besides, there is a need for redesigning the BD-RIS pattern for uplink training because of the different constraints on the scattering matrix, which yields different dimensions and structures of the cascaded channel. Thus, it is important to develop new channel estimation strategies with smaller estimation errors, lower overhead, and reduced power consumption for BD-RIS in the near future.

2) *Joint Consideration of Non-ideal Aspects*: Suppose there are mismatches and mutual coupling of antennas, combined with lossy impedance components which is a reality in practical scenarios, then the channel model in the BD-RIS-based system will no longer be a linear function of the scattering matrix as a result of these RF impairments. Consequently, the BF design will get more complicated.

3) *Continuous, Discrete, and Quantized Phase-shift Designs*: A promising avenue for future research involves a comprehensive investigation of phase-shift design strategies in BD-RIS-aided systems. While continuous phase-shift design offers optimal performance, it is impractical due to hardware limitations. Discrete phase-shift design provides a trade-off between performance and complexity, but it may still require precise control. Quantized phase-shift design, on the other hand, can significantly reduce hardware complexity but may lead to performance degradation. Future research should explore hybrid approaches that combine the advantages of these strategies, such as using continuous phase-shift design for critical elements and quantized phase-shift design for less sensitive elements. Additionally, with the aid of advanced machine learning (ML) algorithms, adaptive phase-shift design algorithms can be developed to dynamically adjust phase-shift values based on channel conditions and system requirements.

4) *Near-field vs. Far-field Propagation*: Integrating BD-RIS in the near-field poses significant challenges due to the rapid variation of the electromagnetic field in this region. Accurate channel estimation and precise control of the BD-RIS elements are crucial to effectively manipulate the wavefronts. Additionally, the design of compact and reconfigurable BD-RIS elements is essential to accommodate the near-field's unique characteristics. For example, in a near-field WPT scenario, BD-RIS could be used to focus the energy towards the receiver, but this requires precise control of the phase shifts to compensate for the rapid phase variations. In contrast, BD-RIS implementation in the far-field is relatively simpler as the wavefronts are planar and the channel characteristics are more predictable. Here, BD-RIS can be used to create virtual LoS paths, enhance signal coverage, and improve the network EE.

5) *Modeling the Inter-Sector Interference of Multi-sector BD-RIS-based Systems*: The representative work in [125] assumes that every BD-RIS antenna has a perfect unidirectional



radiation pattern with no overlaps between the various BD-RIS sectors. In real-world applications, nevertheless, the BD-RIS antennas may have strong sidelobes that result in overlaps, covering users by more than one BD-RIS sector altogether. It is necessary to explore fresh perspectives for imperfect BD-RIS models since the BF design and analysis based on the ideal model will no longer hold when this effect is taken into consideration.

### B. Future Research Directions

The recently proposed BD-RIS-based system has been the subject of decent research activities. However, to optimize the system's benefits, further research areas could be investigated. This subsection describes some of these potential future research areas.

1) *Active vs. Passive BD-RIS Structures*: A research area to be considered will be the comparative performance analyses between the passive elements-based BD-RIS and active elements-based BD-RIS systems. The fundamental tradeoffs in terms of performance, EE, and computational complexity cost for these two BD-RIS alternatives need further investigation.

2) *Integration with Additional Emerging Wireless Technologies*: Exploring the potential uses of BD-RIS models through integration with additional emerging technologies (Other than the ones discussed in Section V-C). In optical wireless communication (OWC), BD-RIS can enhance signal quality and extend coverage by precisely controlling the reflection and refraction of light beams. For D2D communications, BD-RIS can facilitate efficient resource allocation and interference mitigation, leading to improved throughput and reduced latency. In CRN, BD-RIS can enable dynamic spectrum access and interference avoidance, optimizing spectrum utilization. Vehicular Communications can benefit from BD-RIS-assisted signal reflection and BF, improving connectivity and enabling advanced applications like autonomous driving. Integrated terrestrial-satellite networks can seamlessly leverage BD-RIS to bridge the gap between terrestrial and satellite networks, enhancing coverage and capacity. High altitude platform station (HAPS) networks can utilize BD-RIS for flexible BF and coverage extension, especially in remote or disaster-affected regions. Underwater Communications can overcome the challenges of signal propagation and attenuation through BD-RIS-assisted signal reflection and focusing. Coordinate multi-point (CoMP) schemes can leverage BD-RIS for coordinated BF and interference suppression, improving the SE and user experience. Finally, Backscatter Communications can benefit from BD-RIS-assisted energy harvesting and backscattering, enabling low-power devices to communicate efficiently.

3) *Utilizing Advanced Signal Processing Tools to Optimize BD-RIS-based Systems*: There are some new advanced signal processing tools, whose applications on BD-RIS technology will make a difference in terms of performance and implementation. Two prominent of these include both advanced ML and quantum computing (QC). ML techniques, unlike traditional model-based approaches, rely on data-driven models, eliminating the need for precise system-level modeling. Advanced ML techniques, such as federated learning, meta-learning,

graph learning, transfer learning, and quantum learning, can be applied to BD-RIS-based systems to efficiently optimize the configuration of BD-RIS elements due to their massive number. In addition, advanced ML can be used to acquire CSI, perform signal detection, and other signal processing requirements for the optimum performance of BD-RIS. Significant advancements in QC algorithms and hardware in recent years offer a new paradigm for tackling challenging computational issues. In BD-RIS-based wireless communications systems, QC techniques can be used to get around the anticipated high computational optimization complexity related to the BD-RIS-assisted smart radio environment. This can be achieved by recasting the BD-RIS-aided wireless and/or electromagnetic problem into a physical formulation that can be effectively addressed with newly developed QC hardware [144].

4) *Deploying a Transmissive BD-RIS at the Receiver*: BD-RISs offer enhanced flexibility in wave manipulation compared to D-RIS, enabling improved wireless communications performance. While BD-RIS structures are commonly deployed in the channel or at the transmitter side, positioning it at the receiver side presents additional advantages. Strategically placing a transmissive BD-RIS structure at the receiver would enhance the signal reception and empower the receiver to actively shape the incoming signals, leading to significant improvements in overall system performance and user experience. To realize these benefits, the BD-RIS structure must be compact enough to be integrated into receiver devices without compromising their form factor or functionality. However, deploying BD-RIS at the receiver also presents certain challenges. These include the need for precise control and synchronization between the transmitter and the receiver, as well as the potential for increased hardware complexity and power consumption at the receiver. Overcoming these challenges will be essential to fully harness the potential of BD-RIS in future wireless communications systems. Also, the joint deployment of BD-RIS structures in both the channel and in the receiver is an interesting area of future research, similar to the research efforts that investigated such a joint deployment with the D-RIS technology [145].

5) *Prototyping/Experimentation*: Thus far, none of the BD-RIS architectures has been physically realized. Important open research topics include the physical realization of BD-RIS architectures and the associated experimental measurements. Different practical limits of the various BD-RIS architectures (i.e., group-/fully-/tree-/forest-connected and cell-wise single-/group-/dynamically group-/fully-connected) need to be documented, and this will require further investigation while considering real-time scenario issues. Therefore, to experimentally evaluate their benefits in terms of performance enhancement, prototyping of the BD-RIS should be considered. Similarly, the designing of efficient reconfigurable impedance networks with reduced circuit complexity and costs should be explored.

6) *Development of Standards for the BD-RIS Technology*: According to the international mobile telecommunications-2030 "Future Technology Trends" report [146] developed by the international telecommunications union - radio communications sector, RIS is included as technology to enhance radio interface. In September 2021, the industry specifica-

tion group (ISG) on RIS technology was established by the European telecommunications standards institute (ETSI) to facilitate the formal standardization of RISs. According to [147], the analysis of the RIS technology potential, validation, maturity deadlines, and standardization requirements were carried out in ISG's first phase, which ran from 2022 to 2023. Within 2024 and 2025, preliminary guidelines for the RIS technology together with potential group specifications for its functional architecture are scheduled. In the third and final phase of the ISG, which will run from 2026 to 2027, the various RIS solutions will be considered mature. Since consideration regarding standards for the traditional RIS is still ongoing, it may be worthwhile to incorporate BD-RIS into any standard that will eventually be approved for the traditional RIS. In this regard, it is worth noting that the ETSI on one of their reports about the traditional RIS briefly discussed BD-RIS in Section 5.2.1.1 that entitled "Impedance-based structures" [148].

## VII. CONCLUSION

RISs, a well-known candidate technology under investigation for 6G, offers the potential to enhance the efficiency of wireless communications in ways that are both cost-effective and energy-efficient. The analysis of the RIS technology potential, validation, maturity deadlines, and standardization requirements are still under consideration by different interest groups. Its simple architecture and limitations have given rise to a brand-new RIS super-set called BD-RIS. We have started by providing the differences between the D-RIS structure and the BD-RIS structures in terms of design, modeling, limitations, and merits. Then, we have classified the BD-RIS according to its scattering matrix types, modes of transmission, inter-cell architectures, and circuit topologies. Afterward, we have explored some potential applications of BD-RIS that can help in addressing contemporary communications challenges. Next, we have focused on the overview of research progress made in BD-RIS in terms of architectural development, evaluation, and its integration with emerging wireless technologies. Finally, we have discussed some key challenges and future research directions of BD-RIS-aided wireless systems. This survey aims to provide an up-to-date comprehensive review of BD-RIS development and to aid researchers and professionals in accelerating the theoretical investigation and practical implementation of this technology in cutting-edge wireless networks.

## REFERENCES

- [1] Z. Zhang, Y. Xiao, Z. Ma, M. Xiao, Z. Ding, X. Lei, G. K. Karagiannidis, and P. Fan, "6G wireless networks: Vision, requirements, architecture, and key technologies," *IEEE Veh. Technol. Mag.*, vol. 14, no. 3, pp. 28–41, Sep. 2019.
- [2] W. Saad, M. Bennis, and M. Chen, "A vision of 6G wireless systems: Applications, trends, technologies, and open research problems," *IEEE Netw.*, vol. 34, no. 3, pp. 134–142, May 2020.
- [3] C.-X. Wang, X. You, X. Gao, X. Zhu, Z. Li, C. Zhang, H. Wang, Y. Huang, Y. Chen, H. Haas, J. S. Thompson, E. G. Larsson, M. D. Renzo, W. Tong, P. Zhu, X. Shen, H. V. Poor, and L. Hanzo, "On the road to 6G: Visions, requirements, key technologies, and testbeds," *IEEE Commun. Surv. Tutor.*, vol. 25, no. 2, pp. 905–974, 2nd Quart. 2023.
- [4] M. Di Renzo, A. Zappone, M. Debbah, M.-S. Alouini, C. Yuen, J. de Rosny, and S. Tretjakov, "Smart radio environments empowered by reconfigurable intelligent surfaces: How it works, state of research, and the road ahead," *IEEE J. Sel. Areas Commun.*, vol. 38, no. 11, pp. 2450–2525, Nov. 2020.
- [5] Q. Wu and R. Zhang, "Intelligent reflecting surface enhanced wireless network via joint active and passive beamforming," *IEEE Trans. Wirel. Commun.*, vol. 18, no. 11, pp. 5394–5409, Nov. 2019.
- [6] Y. Liu, X. Liu, X. Mu, T. Hou, J. Xu, M. Di Renzo, and N. Al-Dhahir, "Reconfigurable intelligent surfaces: Principles and opportunities," *IEEE Commun. Surv. Tutor.*, vol. 23, no. 3, pp. 1546–1577, 3rd Quart. 2021.
- [7] N. S. Perovic, M. D. Renzo, and M. F. Flanagan, "Channel capacity optimization using reconfigurable intelligent surfaces in indoor mmWave environments," in *IEEE Int. Conf. Commun. (ICC), Dublin, Ireland*, Jun. 2020, pp. 1–7.
- [8] S. Zhou, W. Xu, K. Wang, M. Di Renzo, and M.-S. Alouini, "Spectral and energy efficiency of IRS-assisted MISO communication with hardware impairments," *IEEE Wirel. Commun. Lett.*, vol. 9, no. 9, pp. 1366–1369, Sep. 2020.
- [9] C. Huang, S. Hu, G. C. Alexandropoulos, A. Zappone, C. Yuen, R. Zhang, M. D. Renzo, and M. Debbah, "Holographic MIMO surfaces for 6G wireless networks: Opportunities, challenges, and trends," *IEEE Wirel. Commun.*, vol. 27, no. 5, pp. 118–125, Oct. 2020.
- [10] Q. Ding, J. Yang, Y. Luo, and C. Luo, "Intelligent reflecting surface vs. conventional full-duplex relay in mmWave MIMO networks: A comprehensive performance comparison," *IEEE Trans. Veh. Technol.*, vol. 73, no. 11, pp. 17 231–17 246, Nov. 2024.
- [11] S. Gong, X. Lu, D. T. Hoang, D. Niyato, L. Shu, D. I. Kim, and Y.-C. Liang, "Toward smart wireless communications via intelligent reflecting surfaces: A contemporary survey," *IEEE Commun. Surv. Tutor.*, vol. 22, no. 4, pp. 2283–2314, 4th Quart. 2020.
- [12] W. U. Khan, E. Lagunas, A. Mahmood, M. Asif, M. Ahmed, and S. Chatzinotas, "Integration of beyond diagonal RIS and UAVs in 6G NTN: Enhancing aerial connectivity," *arXiv preprint arXiv:2409.06073*, Sep. 2024.
- [13] E. Basar, M. Di Renzo, J. De Rosny, M. Debbah, M.-S. Alouini, and R. Zhang, "Wireless communications through reconfigurable intelligent surfaces," *IEEE Access*, vol. 7, pp. 116 753–116 773, 2019.
- [14] M. Ahmed, S. Raza, A. A. Soofi, F. Khan, W. U. Khan, S. Z. U. Abideen, F. Xu, and Z. Han, "Active reconfigurable intelligent surfaces: Expanding the frontiers of wireless communication-A survey," *IEEE Commun. Surv. Tutor.*, pp. 1–1, early access, 2024.
- [15] Q. Wu and R. Zhang, "Towards smart and reconfigurable environment: Intelligent reflecting surface aided wireless network," *IEEE Commun. Mag.*, vol. 58, no. 1, pp. 106–112, Jan. 2020.
- [16] R. K. Fotock, A. Zappone, and M. D. Renzo, "Energy efficiency optimization in RIS-aided wireless networks: Active versus nearly-passive RIS with global reflection constraints," *IEEE Trans. Commun.*, vol. 72, no. 1, pp. 257–272, Jan. 2024.
- [17] C. Pan, H. Ren, K. Wang, J. F. Kolb, M. Elkhachan, M. Chen, M. Di Renzo, Y. Hao, J. Wang, A. L. Swindlehurst, X. You, and L. Hanzo, "Reconfigurable intelligent surfaces for 6G systems: Principles, applications, and research directions," *IEEE Commun. Mag.*, vol. 59, no. 6, pp. 14–20, Jun., 2021.
- [18] M. H. Khoshafa, T. M. N. Ngatched, M. H. Ahmed, and A. R. Ndjiongue, "Active reconfigurable intelligent surfaces-aided wireless communication system," *IEEE Commun. Lett.*, vol. 25, no. 11, pp. 3699–3703, Nov. 2021.
- [19] Z. Zhang, L. Dai, X. Chen, C. Liu, F. Yang, R. Schober, and H. V. Poor, "Active RIS vs. passive RIS: Which will prevail in 6G?" *IEEE Trans. Commun.*, vol. 71, no. 3, pp. 1707–1725, Mar. 2023.
- [20] A. Taha, M. Alrabeiah, and A. Alkhateeb, "Enabling large intelligent surfaces with compressive sensing and deep learning," *IEEE Access*, vol. 9, pp. 44 304–44 321, Jan. 2021.
- [21] G. C. Alexandropoulos and E. Vlachos, "A hardware architecture for reconfigurable intelligent surfaces with minimal active elements for explicit channel estimation," in *IEEE Int. Conf. Acoust. Speech Signal Process. (ICASSP), Barcelona, Spain*, May 2020, pp. 9175–9179.
- [22] Y. Liu, X. Mu, J. Xu, R. Schober, Y. Hao, H. V. Poor, and L. Hanzo, "STAR: Simultaneous transmission and reflection for 360° coverage by intelligent surfaces," *IEEE Wirel. Commun.*, vol. 28, no. 6, pp. 102–109, Dec. 2021.
- [23] H. Zhang, S. Zeng, B. Di, Y. Tan, M. Di Renzo, M. Debbah, Z. Han, H. V. Poor, and L. Song, "Intelligent omni-surfaces for full-dimensional wireless communications: Principles, technology, and implementation," *IEEE Commun. Mag.*, vol. 60, no. 2, pp. 39–45, Feb. 2022.

- [24] M. H. Khoshafa, T. M. Ngatched, M. H. Ahmed, and Y. Gadallah, "RIS-empowered rate-splitting multiple access towards 6G and beyond wireless communications networks: A comprehensive survey," *Authorea Preprints*, Feb. 2025.
- [25] M. H. Khoshafa, F. Bueno, T. M. Ngatched, and M. Di Renzo, "RIS-empowered secured space-air-ground integrated networks: Opportunities and challenges," *Authorea Preprints*, Feb. 2025.
- [26] C. Liaskos, S. Nie, A. Tsioliaridou, A. Pitsillides, S. Ioannidis, and I. Akyildiz, "A new wireless communication paradigm through software-controlled metasurfaces," *IEEE Commun. Mag.*, vol. 56, no. 9, pp. 162–169, Sep. 2018.
- [27] M. H. Khoshafa, Y. Gadallah, T. M. N. Ngatched, and M. H. Ahmed, "Aerial reconfigurable intelligent surface-assisted LPWANs for IoT: A cross-layer analysis," *IEEE Wirel. Commun. Lett.*, vol. 13, no. 10, pp. 2912–2916, Oct. 2024.
- [28] H. Yahya, H. Li, M. Nerini, B. Clerckx, and M. Debbah, "Beyond diagonal RIS: Passive maximum ratio transmission and interference nulling enabler," *IEEE Open J. Commun. Soc.*, vol. 5, pp. 7613–7627, 2024.
- [29] W. Sun, S. Sun, T. Shi, X. Su, and R. Liu, "A new model of beyond diagonal reconfigurable intelligent surfaces (BD-RIS) for the corresponding quantization and optimization," *IEEE Trans. Wirel. Commun.*, vol. 23, no. 9, pp. 11 521–11 534, Sep. 2024.
- [30] H. Alakoca, M. Namdar, S. Aldirmaz-Colak, M. Basaran, A. Basgumus, L. Durak-Ata, and H. Yanikomeroglu, "Metasurface manipulation attacks: Potential security threats of RIS-aided 6G communications," *IEEE Commun. Mag.*, vol. 61, no. 1, pp. 24–30, Jan. 2023.
- [31] H. Li, S. Shen, M. Nerini, and B. Clerckx, "Reconfigurable intelligent surfaces 2.0: Beyond diagonal phase shift matrices," *IEEE Commun. Mag.*, vol. 62, no. 3, pp. 102–108, Mar. 2024.
- [32] S. Shen, B. Clerckx, and R. Murch, "Modeling and architecture design of reconfigurable intelligent surfaces using scattering parameter network analysis," *IEEE Trans. Wirel. Commun.*, vol. 21, no. 2, pp. 1229–1243, Feb. 2022.
- [33] M. Nerini, S. Shen, H. Li, M. D. Renzo, and B. Clerckx, "A universal framework for multipoint network analysis of reconfigurable intelligent surfaces," *IEEE Trans. Wirel. Commun.*, vol. 23, no. 10, pp. 14 575–14 590, Oct. 2024.
- [34] P. Del Hougne, "Physics-compliant diagonal representation of beyond-diagonal RIS," in *IEEE Workshop Signal Process. Adv. Wirel. Commun. (SPAWC)*, Lucca, Italy, Sep. 2024, pp. 931–935.
- [35] P. del Hougne, "A physics-compliant diagonal representation for wireless channels parametrized by beyond-diagonal reconfigurable intelligent surfaces," *arXiv preprint arXiv:2409.20509*, Sep. 2024.
- [36] M. Nerini, S. Shen, H. Li, and B. Clerckx, "Beyond diagonal reconfigurable intelligent surfaces utilizing graph theory: Modeling, architecture design, and optimization," *IEEE Trans. Wirel. Commun.*, vol. 23, no. 8, pp. 9972–9985, Aug. 2024.
- [37] M. T. Ivrlac and J. A. Nossek, "Toward a circuit theory of communication," *IEEE Trans. Circuits Syst. I: Regul. Pap.*, vol. 57, no. 7, pp. 1663–1683, Jul. 2010.
- [38] H. Li, M. Nerini, S. Shen, and B. Clerckx, "Wideband modeling and beamforming for beyond diagonal reconfigurable intelligent surfaces," in *IEEE Workshop Signal Process. Adv. Wirel. Commun. (SPAWC)*, Lucca, Italy, Sep. 2024, pp. 926–930.
- [39] H. Li, M. Nerini, S. Shen, and B. Clerckx, "Beyond diagonal reconfigurable intelligent surfaces in wideband OFDM communications: Circuit-based modeling and optimization," *IEEE Trans. Wirel. Commun.*, pp. 1–1, early access, 2025.
- [40] W. Xu and S. Qiao, "A divide-and-conquer method for the Takagi factorization," *SIAM J. Matrix Anal. Appl.*, vol. 30, no. 1, pp. 142–153, 2008.
- [41] W. U. Khan, A. Mahmood, M. A. Jamshed, E. Lagunas, M. Ahmed, and S. Chatzinotas, "Beyond diagonal RIS for 6G non-terrestrial networks: Potentials and challenges," *IEEE Netw.*, vol. 39, no. 1, pp. 80–89, Jan. 2025.
- [42] M. Ahmed, F. Xu, A. Wahid, K. Ali, M. A. Mirza, W. Khan, K. Dev, S. A. Hassan, and Z. Han, "A comprehensive survey of artificial intelligence advances in RIS-assisted wireless networks," *Authorea Preprints*, Aug. 2024.
- [43] H. Li, S. Shen, and B. Clerckx, "Beyond diagonal reconfigurable intelligent surfaces: From transmitting and reflecting modes to single-, group-, and fully-connected architectures," *IEEE Trans. Wirel. Commun.*, vol. 22, no. 4, pp. 2311–2324, Apr. 2023.
- [44] W. U. Khan, E. Lagunas, and S. Chatzinotas, "Transmissive beyond diagonal RIS-mounted LEO communication for NOMA IoT networks," *arXiv preprint arXiv:2501.02742*, Jan. 2025.
- [45] M. Nerini and B. Clerckx, "Physically consistent modeling of stacked intelligent metasurfaces implemented with beyond diagonal RIS," *IEEE Commun. Lett.*, vol. 28, no. 7, pp. 1693–1697, Jul. 2024.
- [46] H. Li, S. Shen, and B. Clerckx, "A dynamic grouping strategy for beyond diagonal reconfigurable intelligent surfaces with hybrid transmitting and reflecting mode," *IEEE Trans. Veh. Tech.*, vol. 72, no. 12, pp. 16 748–16 753, Dec. 2023.
- [47] H. Li, S. Shen, and B. Clerckx, "Beyond diagonal reconfigurable intelligent surfaces: A multi-sector mode enabling highly directional full-space wireless coverage," *IEEE J. Sel. Areas Commun.*, vol. 41, no. 8, pp. 2446–2460, Aug. 2023.
- [48] Y. Dong, Q. Li, S. X. Ng, and M. El-Hajjar, "Reconfigurable intelligent surface relying on low-complexity joint sector non-diagonal structure," *IEEE Open J. Veh. Technol.*, vol. 5, pp. 1106–1123, 2024.
- [49] Q. Li, M. El-Hajjar, I. Hemadeh, A. Shojaeifard, A. A. M. Mourad, B. Clerckx, and L. Hanzo, "Reconfigurable intelligent surfaces relying on non-diagonal phase shift matrices," *IEEE Trans. Veh. Tech.*, vol. 71, no. 6, pp. 6367–6383, Jun. 2022.
- [50] K. Chen and Y. Mao, "Transmitter side beyond-diagonal RIS for mmWave integrated sensing and communications," in *IEEE Workshop Signal Process. Adv. Wirel. Commun. (SPAWC)*, Lucca, Italy, Sep. 2024, pp. 951–955.
- [51] M. Samy, A. B. M. Adam, K. Ntontin, H. Al-Hraishawi, S. Chatzinotas, and B. Ottersten, "Enhancing spectral and energy efficiency with multi-sector beyond-diagonal RIS," in *IEEE Workshop Signal Process. Adv. Wirel. Commun. (SPAWC)*, Lucca, Italy, Sep. 2024, pp. 941–945.
- [52] S. Zhang, H. Zhang, B. Di, Y. Tan, Z. Han, and L. Song, "Beyond intelligent reflecting surfaces: Reflective-transmissive metasurface aided communications for full-dimensional coverage extension," *IEEE Trans. Veh. Tech.*, vol. 69, no. 11, pp. 13 905–13 909, Nov. 2020.
- [53] M. H. Khoshafa, O. Maraqa, J. M. Moualeu, S. Aboagye, T. M. N. Ngatched, M. H. Ahmed, Y. Gadallah, and M. D. Renzo, "RIS-assisted physical layer security in emerging RF and optical wireless communication systems: A comprehensive survey," *IEEE Commun. Surv. Tutor.*, pp. 1–1, early access, 2024.
- [54] M. H. Khoshafa, T. M. N. Ngatched, and M. H. Ahmed, "Reconfigurable intelligent surfaces-aided physical layer security enhancement in D2D underlay communications," *IEEE Commun. Lett.*, vol. 25, no. 5, pp. 1443–1447, May 2021.
- [55] M. H. Khoshafa, G. Ahmed, T. M. N. Ngatched, and M. D. Renzo, "Aerial reconfigurable intelligent surfaces-enabled secured wireless communications: Performance analysis and optimization," *IEEE Trans. Commun.*, pp. 1–1, early access, 2024.
- [56] M. H. Khoshafa, T. M. N. Ngatched, Y. Gadallah, and M. H. Ahmed, "Securing lpwans: A reconfigurable intelligent surface (RIS)-assisted UAV approach," *IEEE Wireless Comm. Lett.*, vol. 13, no. 1, pp. 158–162, Jan. 2024.
- [57] M. H. Khoshafa, T. M. N. Ngatched, and M. H. Ahmed, "RIS-aided physical layer security improvement in underlay cognitive radio networks," *IEEE Sys. J.*, vol. 17, no. 4, pp. 6437–6448, Dec. 2023.
- [58] R. Borralho, A. Mohamed, A. U. Qudus, P. Vieira, and R. Tafazolli, "A survey on coverage enhancement in cellular networks: Challenges and solutions for future deployments," *IEEE Commun. Surv. Tutor.*, vol. 23, no. 2, pp. 1302–1341, 2nd Quart. 2021.
- [59] A. S. De Sena, M. Rasti, N. H. Mahmood, and M. Latva-aho, "Beyond diagonal RIS for multi-band multi-cell MIMO networks: A practical frequency-dependent model and performance analysis," *IEEE Trans. Wirel. Commun.*, vol. 24, no. 1, pp. 749–766, Jan. 2025.
- [60] F. Liu, Y. Cui, C. Masouros, J. Xu, T. X. Han, Y. C. Eldar, and S. Buzzi, "Integrated sensing and communications: Toward dual-functional wireless networks for 6G and beyond," *IEEE J. Sel. Areas Commun.*, vol. 40, no. 6, pp. 1728–1767, Jun. 2022.
- [61] Y. Cui, F. Liu, X. Jing, and J. Mu, "Integrating sensing and communications for ubiquitous IoT: Applications, trends, and challenges," *IEEE Netw.*, vol. 35, no. 5, pp. 158–167, Oct. 2021.
- [62] A. Liu, Z. Huang, M. Li, Y. Wan, W. Li, T. X. Han, C. Liu, R. Du, D. K. P. Tan, J. Lu, Y. Shen, F. Colone, and K. Chetty, "A survey on fundamental limits of integrated sensing and communication," *IEEE Commun. Surv. Tutor.*, vol. 24, no. 2, pp. 994–1034, 2nd Quart. 2022.
- [63] Z. Liu, Y. Liu, S. Shen, Q. Wu, and Q. Shi, "Enhancing ISAC network throughput using beyond diagonal RIS," *IEEE Wirel. Commun. Lett.*, vol. 13, no. 6, pp. 1670–1674, Jun. 2024.
- [64] Z. Guang, Y. Liu, Q. Wu, W. Wang, and Q. Shi, "Power minimization for ISAC system using beyond diagonal reconfigurable intelligent surface," *IEEE Trans. Veh. Tech.*, vol. 73, no. 9, pp. 13 950–13 955, Sep. 2024.

- [65] T. Esmaeilbeig, K. V. Mishra, and M. Soltanalian, "Beyond diagonal RIS: Key to next-generation integrated sensing and communications?" *IEEE Signal Process. Lett.*, vol. 32, pp. 216–220, 2025.
- [66] M. Nerini, G. Ghiaasi, and B. Clerckx, "Localized and distributed beyond diagonal reconfigurable intelligent surfaces with lossy interconnections: Modeling and optimization," *IEEE Trans. Commun.*, pp. 1–1, early access, 2025.
- [67] B. Wang, H. Li, S. Shen, Z. Cheng, and B. Clerckx, "A dual-function radar-communication system empowered by beyond diagonal reconfigurable intelligent surface," *IEEE Trans. Commun.*, pp. 1–1, early access, 2024.
- [68] M. Raeisi, H. Chen, H. Wymeersch, and E. Basar, "Efficient localization with base station-integrated beyond diagonal RIS," *arXiv preprint arXiv:2411.13295*, Nov. 2024.
- [69] S. Zheng, B. Lv, T. Zhang, Y. Xu, G. Chen, R. Wang, and P. C. Ching, "On DoF of active RIS-assisted MIMO interference channel with arbitrary antenna configurations: When will RIS help?" *IEEE Trans. Veh. Technol.*, vol. 72, no. 12, pp. 16 828–16 833, Dec. 2023.
- [70] M. A. ElMossallamy, H. Zhang, R. Sultan, K. G. Seddik, L. Song, G. Y. Li, and Z. Han, "On spatial multiplexing using reconfigurable intelligent surfaces," *IEEE Wirel. Commun. Lett.*, vol. 10, no. 2, pp. 226–230, Feb. 2021.
- [71] A. H. A. Bafghi, V. Jamali, M. Nasiri-Kenari, and R. Schober, "Degrees of freedom of the  $k$ -user interference channel assisted by active and passive IRSs," *IEEE Trans. Commun.*, vol. 70, no. 5, pp. 3063–3080, May 2022.
- [72] S. Meng, W. Tang, W. Chen, J. Lan, Q. Y. Zhou, Y. Han, X. Li, and S. Jin, "Rank optimization for MIMO channel with RIS: Simulation and measurement," *IEEE Wirel. Commun. Lett.*, vol. 13, no. 2, pp. 437–441, Feb. 2024.
- [73] Y. Zhao, H. Li, M. Franceschetti, and B. Clerckx, "Channel shaping using beyond diagonal reconfigurable intelligent surface: Analysis, optimization, and enhanced flexibility," *arXiv preprint arXiv:2407.15196*, Jul. 2024.
- [74] J. V. Alegría, J. Thunberg, and O. Edfors, "Channel orthogonalization with reconfigurable surfaces: General models, theoretical limits, and effective configuration," *arXiv preprint arXiv:2403.15165*, Mar. 2024.
- [75] A. Papazafeiropoulos, P. Kourtessis, and S. Chatzinotas, "Effect of channel aging on beyond diagonal reconfigurable intelligent surfaces," *IEEE Open J. Commun. Soc.*, vol. 5, pp. 6303–6313, 2024.
- [76] N. U. Hassan, J. An, M. Di Renzo, M. Debbah, and C. Yuen, "Efficient beamforming and radiation pattern control using stacked intelligent metasurfaces," *IEEE Open J. Commun. Society*, vol. 5, pp. 599–611, 2024.
- [77] A. Papazafeiropoulos, J. An, P. Kourtessis, T. Ratnarajah, and S. Chatzinotas, "Achievable rate optimization for stacked intelligent metasurface-assisted holographic MIMO communications," *IEEE Trans. Wirel. Commun.*, vol. 23, no. 10, pp. 13 173–13 186, Oct. 2024.
- [78] J. An, C. Yuen, C. Xu, H. Li, D. W. K. Ng, M. Di Renzo, M. Debbah, and L. Hanzo, "Stacked intelligent metasurface-aided MIMO transceiver design," *IEEE Wirel. Commun.*, vol. 31, no. 4, pp. 123–131, Aug. 2024.
- [79] J. Xu, Y. Liu, X. Mu, and O. A. Dobre, "STAR-RISs: Simultaneous transmitting and reflecting reconfigurable intelligent surfaces," *IEEE Commun. Lett.*, vol. 25, no. 9, pp. 3134–3138, Sep. 2021.
- [80] J. Xu, Y. Liu, X. Mu, J. T. Zhou, L. Song, H. V. Poor, and L. Hanzo, "Simultaneously transmitting and reflecting intelligent omni-surfaces: Modeling and implementation," *IEEE Veh. Tech. Mag.*, vol. 17, no. 2, pp. 46–54, Jun. 2022.
- [81] H. Wang, Z. Han, and A. L. Swindlehurst, "Channel reciprocity attacks using intelligent surfaces with non-diagonal phase shifts," *IEEE Open J. Commun. Soc.*, vol. 5, pp. 1469–1485, 2024.
- [82] H. Wang, J. Nassek, and A. L. Swindlehurst, "Beyond-diagonal RIS attacks on physical layer key generation," in *IEEE Workshop Signal Process. Adv. Wirel. Commun. (SPAWC)*, Lucca, Italy, Sep. 2024, pp. 946–950.
- [83] Y. Zhang, X. Shao, H. Li, B. Clerckx, and R. Zhang, "Full-space wireless sensing enabled by multi-sector intelligent surfaces," *arXiv preprint arXiv:2406.15945*, Jun. 2024.
- [84] A. Mishra, Y. Mao, C. D'Andrea, S. Buzzi, and B. Clerckx, "Transmitter side beyond-diagonal reconfigurable intelligent surface for massive MIMO networks," *IEEE Wirel. Commun. Lett.*, vol. 13, no. 2, pp. 352–356, Feb. 2024.
- [85] K. D. Katsanos, P. D. Lorenzo, and G. C. Alexandropoulos, "Multi-RIS-empowered multiple access: A distributed sum-rate maximization approach," *IEEE J. Sel. Top. Signal Process.*, vol. 18, no. 7, pp. 1324–1338, Oct. 2024.
- [86] Q. Li, M. El-Hajjar, I. Hemadeh, A. Shojaefard, and L. Hanzo, "Coordinated reconfigurable intelligent surfaces: Non-diagonal group-connected design," *IEEE Trans. Veh. Tech.*, vol. 73, no. 7, pp. 10 811–10 816, Jul. 2024.
- [87] M. Nerini, S. Shen, and B. Clerckx, "Static grouping strategy design for beyond diagonal reconfigurable intelligent surfaces," *IEEE Commun. Lett.*, vol. 28, no. 7, pp. 1708–1712, Jul. 2024.
- [88] H. Li, S. Shen, M. Nerini, M. Di Renzo, and B. Clerckx, "Beyond diagonal reconfigurable intelligent surfaces with mutual coupling: Modeling and optimization," *IEEE Commun. Lett.*, vol. 28, no. 4, pp. 937–941, Apr. 2024.
- [89] M. Nerini, H. Li, and B. Clerckx, "Global optimal closed-form solutions for intelligent surfaces with mutual coupling: Is mutual coupling detrimental or beneficial?" *arXiv preprint arXiv:2411.04949*, Nov. 2024.
- [90] H. Li and B. Clerckx, "Non-reciprocal beyond diagonal RIS: Multipoint network models and performance benefits in full-duplex systems," *arXiv preprint arXiv:2411.04370*, Nov. 2024.
- [91] Z. Liu, H. Li, and B. Clerckx, "Non-reciprocal beyond diagonal RIS: Sum-rate maximization in full-duplex communications," *arXiv preprint arXiv:2411.18523*, Dec. 2024.
- [92] M. Nerini, S. Shen, and B. Clerckx, "Discrete-value group and fully connected architectures for beyond diagonal reconfigurable intelligent surfaces," *IEEE Trans. Veh. Tech.*, vol. 72, no. 12, pp. 16 354–16 368, Dec. 2023.
- [93] M. Nerini and B. Clerckx, "Dual-polarized beyond diagonal RIS," *arXiv preprint arXiv:2412.16097*, Dec. 2024.
- [94] X. Zhou, T. Fang, and Y. Mao, "A novel Q-stem connected architecture for beyond-diagonal reconfigurable intelligent surfaces," *arXiv preprint arXiv:2411.18480*, Nov. 2024.
- [95] H. Li, Y. Zhang, and B. Clerckx, "Channel estimation for beyond diagonal reconfigurable intelligent surfaces with group-connected architectures," in *IEEE Int. Workshop Comput. Adv. Multi-Sensor Adaptive Process. (CAMSAP)*, Herradura, Costa Rica, Dec. 2023, pp. 21–25.
- [96] H. Li, S. Shen, Y. Zhang, and B. Clerckx, "Channel estimation and beamforming for beyond diagonal reconfigurable intelligent surfaces," *IEEE Trans. Signal Process.*, vol. 72, pp. 3318–3332, 2024.
- [97] A. L. de Almeida, B. Sokal, H. Li, and B. Clerckx, "Channel estimation for beyond diagonal RIS via tensor decomposition," *arXiv preprint arXiv:2407.20402*, Jul. 2024.
- [98] B. Sokal, A. L. de Almeida, H. Li, B. Clerckx *et al.*, "A decoupled channel estimation method for beyond diagonal RIS," *arXiv preprint arXiv:2412.06683*, Dec. 2024.
- [99] N. Ginige, A. S. de Sena, N. H. Mahmood, N. Rajatheva, and M. Latvaaho, "Efficient channel prediction for beyond diagonal RIS-assisted MIMO systems with channel aging," *arXiv preprint arXiv:2411.17725*, Nov. 2024.
- [100] M. Soleymani, I. Santamaria, A. Sezgin, and E. Jorswieck, "Maximizing spectral and energy efficiency in multi-user MIMO OFDM systems with RIS and hardware impairment," *arXiv preprint arXiv:2401.11921*, Jan. 2024.
- [101] M. Samy, H. Al-Hraishawi, A. B. M. Adam, S. Chatzinotas, and B. Ottersten, "Beyond diagonal RIS-aided networks: Performance analysis and sectorization tradeoff," *IEEE Open J. Commun. Soc.*, vol. 6, pp. 302–315, 2025.
- [102] T. Fang and Y. Mao, "A low-complexity beamforming design for beyond-diagonal RIS aided multi-user networks," *IEEE Commun. Lett.*, vol. 28, no. 1, pp. 203–207, Jan. 2024.
- [103] M. Nerini and B. Clerckx, "Pareto frontier for the performance-complexity trade-off in beyond diagonal reconfigurable intelligent surfaces," *IEEE Commun. Lett.*, vol. 27, no. 10, pp. 2842–2846, Oct. 2023.
- [104] M. Nerini, S. Shen, and B. Clerckx, "Closed-form global optimization of beyond diagonal reconfigurable intelligent surfaces," *IEEE Trans. Wirel. Commun.*, vol. 23, no. 2, pp. 1037–1051, Feb. 2024.
- [105] Y. Zhou, Y. Liu, H. Li, Q. Wu, S. Shen, and B. Clerckx, "Optimizing power consumption, energy efficiency, and sum-rate using beyond diagonal RIS-a unified approach," *IEEE Trans. Wirel. Commun.*, vol. 23, no. 7, pp. 7423–7438, Jul. 2024.
- [106] Z. Wu and B. Clerckx, "Optimization of beyond diagonal RIS: A universal framework applicable to arbitrary architectures," *arXiv preprint arXiv:2412.15965*, Dec. 2024.
- [107] I. Santamaria, M. Soleymani, E. Jorswieck, and J. Gutierrez, "SNR maximization in beyond diagonal RIS-assisted single and multiple antenna links," *IEEE Signal Process. Lett.*, vol. 30, pp. 923–926, 2023.
- [108] I. Santamaria, M. Soleymani, E. Jorswieck, and J. Gutierrez, "MIMO capacity maximization with beyond-diagonal RIS," in *IEEE Workshop*

- Signal Process. Adv. Wirel. Commun. (SPAWC), Lucca, Italy*, Sep. 2024, pp. 936–940.
- [109] E. Björnson and Ö. T. Demir, “Capacity maximization for MIMO channels assisted by beyond-diagonal RIS,” *arXiv preprint arXiv:2411.18298*, Nov. 2024.
- [110] K. D. Katsanos, P. Di Lorenzo, and G. C. Alexandropoulos, “The interference broadcast channel with reconfigurable intelligent surfaces: A cooperative sum-rate maximization approach,” in *IEEE Workshop Signal Process. Adv. Wirel. Commun. (SPAWC), Lucca, Italy*, Sep. 2024, pp. 551–555.
- [111] X. Zhou, T. Fang, and Y. Mao, “Joint active and passive beamforming optimization for beyond diagonal RIS-aided multi-user communications,” *IEEE Commun. Lett.*, pp. 1–1, early access, 2025.
- [112] M. Soleymani, A. Zappone, E. Jorswieck, M. D. Renzo, and I. Santamaria, “Rate region of RIS-aided URLLC broadcast channels: Diagonal versus beyond diagonal globally passive RIS,” *IEEE Wirel. Commun. Lett.*, vol. 14, no. 2, pp. 320–324, Feb. 2025.
- [113] M. Soleymani, I. Santamaria, E. Jorswieck, M. Di Renzo, and J. Gutierrez, “Energy efficiency comparison of RIS architectures in MISO broadcast channels,” in *IEEE Workshop Signal Process. Adv. Wirel. Commun. (SPAWC), Lucca, Italy*, Sep. 2024, pp. 701–705.
- [114] J. Singh, S. Srivastava, A. K. Jagannatham, and L. Hanzo, “Joint transceiver and reconfigurable intelligent surface design for multiuser mmWave MIMO systems relying on non-diagonal phase shift matrices,” *IEEE Open J. Commun. Soc.*, vol. 4, pp. 2897–2912, 2023.
- [115] S. Sobhi-Givi, M. Nouri, H. Behroozi, and Z. Ding, “Joint BS and beyond diagonal RIS beamforming design with DRL methods for mmWave 6G mobile communications,” in *IEEE Wirel. Commun. Netw. Conf. (WCNC), Dubai, United Arab Emirates*, Apr. 2024, pp. 1–6.
- [116] W. U. Khan, C. K. Sheemar, Z. Abdullah, E. Lagunas, and S. Chatzinotas, “Beyond diagonal IRS assisted ultra massive THz systems: A low resolution approach,” in *IEEE Int. Symp. Pers. Indoor Mob. Radio Commun. (PIMRC), Valencia, Spain*, Sep. 2024, pp. 1–5.
- [117] A. Mahmood, T. X. Vu, S. Chatzinotas, and B. Ottersten, “Enhancing indoor and outdoor THz communications with beyond diagonal-IRS: Optimization and performance analysis,” in *IEEE 35th IEEE Int. Symp. Pers. Indoor Mob. Radio Commun. (PIMRC), Valencia, Spain*, Sep. 2024, pp. 1–6.
- [118] A. M. Huroon, Y.-C. Huang, and L.-C. Wang, “Optimized transmission strategy for UAV-RIS 2.0 assisted communications using rate splitting multiple access,” in *IEEE Veh. Technol. Conf. (VTC2023-Fall), Hong Kong, Hong Kong*, Oct. 2023, pp. 1–6.
- [119] A. Mahmood, T. X. Vu, W. U. Khan, S. Chatzinotas, and B. Ottersten, “Joint computation and communication resource optimization for beyond diagonal UAV-IRS empowered MEC networks,” *arXiv preprint arXiv:2311.07199*, Nov. 2023.
- [120] X. Peng, Z. Chen, J. Ye, P. Zhang, and L. Huang, “Beyond-diagonal RIS aided DFRC systems: A joint beamforming optimization design method,” in *IEEE/CIC Int. Conf. Commun. in China (ICCC Workshops), Hangzhou, China*, Aug. 2024, pp. 782–787.
- [121] T. D. Hua, M. Mohammadi, H. Q. Ngo, and M. Matthaiou, “Cell-free massive MIMO SWIPT with beyond diagonal reconfigurable intelligent surfaces,” in *IEEE Wirel. Commun. Netw. Conf. (WCNC), Dubai, United Arab Emirates*, Apr. 2024, pp. 1–6.
- [122] A. Azarbahram, O. L. López, B. Clerckx, M. Di Renzo, and M. Latvaaho, “Beyond diagonal reconfigurable intelligent surfaces for multi-carrier RF wireless power transfer,” *arXiv preprint arXiv:2501.01787*, Jan. 2025.
- [123] M. Soleymani, I. Santamaria, E. A. Jorswieck, and B. Clerckx, “Optimization of rate-splitting multiple access in beyond diagonal RIS-assisted URLLC systems,” *IEEE Trans. Wirel. Commun.*, vol. 23, no. 5, pp. 5063–5078, May 2024.
- [124] T. Fang, Y. Mao, S. Shen, Z. Zhu, and B. Clerckx, “Fully connected reconfigurable intelligent surface aided rate-splitting multiple access for multi-user multi-antenna transmission,” in *IEEE Int. Conf. Commun. Workshops (ICC Workshops), Seoul, Korea*, May 2022, pp. 675–680.
- [125] H. Li, S. Shen, and B. Clerckx, “Synergizing beyond diagonal reconfigurable intelligent surface and rate-splitting multiple access,” *IEEE Trans. Wirel. Commun.*, vol. 23, no. 8, pp. 8717–8729, Aug. 2024.
- [126] S. Khisa, A. Amhaz, M. Elhattab, C. Assi, and S. Sharafeddine, “Gradient-based meta learning for uplink RSMA with beyond diagonal RIS,” *arXiv preprint arXiv:2410.17896*, Oct. 2024.
- [127] Q. Zhang, G. Luo, Z. Dong, F. Sun, X. Wang, and J. Liu, “Beyond-diagonal reconfigurable intelligent surface enhanced NOMA systems,” *IEEE Wirel. Commun. Lett.*, vol. 14, no. 1, pp. 118–122, Jan. 2025.
- [128] O. T. Demir and E. Björnson, “Wideband channel capacity maximization with beyond diagonal RIS reflection matrices,” *IEEE Wirel. Commun. Lett.*, vol. 13, no. 10, pp. 2687–2691, Oct. 2024.
- [129] R. C. Loli and B. Clerckx, “Meta-learning based optimization for large scale wireless systems,” *arXiv preprint arXiv:2407.01823*, Jul. 2024.
- [130] C. Zhang, W. U. Khan, A. K. Bashir, A. K. Dutta, A. U. Rehman, and M. M. A. Dabel, “Sum rate maximization for 6G beyond diagonal RIS-assisted multi-cell transportation systems,” *IEEE Trans. Intell. Transp. Syst.*, pp. 1–11, early access, 2025.
- [131] T. Kim, B. Clerckx, D. J. Love, and S. J. Kim, “Limited feedback beamforming systems for dual-polarized MIMO channels,” *IEEE Trans. Wirel. Commun.*, vol. 9, no. 11, pp. 3425–3439, Nov. 2010.
- [132] A. S. Rajasekaran, O. Maraqa, H. U. Sokun, H. Yanikomeroglu, and S. Al-Ahmadi, “User clustering in mmWave-NOMA systems with user decoding capability constraints for b5g networks,” *IEEE Access*, vol. 8, pp. 209 949–209 963, 2020.
- [133] O. Maraqa, A. S. Rajasekaran, H. U. Sokun, S. Al-Ahmadi, H. Yanikomeroglu, and S. M. Sait, “Energy-efficient coverage enhancement of indoor THz-MISO systems: An FD-NOMA approach,” in *IEEE Int. Symp. Pers. Indoor Mob. Radio Commun. (PIMRC), Helsinki, Finland*, Sep. 2021, pp. 483–489.
- [134] O. Maraqa, S. Al-Ahmadi, A. S. Rajasekaran, H. U. Sokun, H. Yanikomeroglu, and S. M. Sait, “Energy-efficient optimization of multi-user NOMA-assisted cooperative THz-SIMO MEC systems,” *IEEE Trans. Commun.*, vol. 71, no. 6, pp. 3763–3779, 2023.
- [135] L. Zheng, M. Lops, Y. C. Eldar, and X. Wang, “Radar and communication coexistence: An overview,” *IEEE Signal Process. Mag.*, vol. 36, no. 5, pp. 85–99, Sep. 2019.
- [136] T. D. Ponnimbaduge Perera, D. N. K. Jayakody, S. K. Sharma, S. Chatzinotas, and J. Li, “Simultaneous wireless information and power transfer (SWIPT): Recent advances and future challenges,” *IEEE Commun. Surv. Tutor.*, vol. 20, no. 1, pp. 264–302, 1st Quart. 2018.
- [137] B. S. Khan, S. Jangsher, A. Ahmed, and A. Al-Dweik, “URLLC and eMBB in 5G industrial IoT: A survey,” *IEEE Open J. Commun. Soc.*, vol. 3, pp. 1134–1163, 2022.
- [138] O. Maraqa, S. Aboagye, and T. M. N. Ngatched, “Optical STAR-RIS-aided VLC systems: RSMA versus NOMA,” *IEEE Open J. Commun. Soc.*, vol. 5, pp. 430–441, 2024.
- [139] O. Maraqa, A. S. Rajasekaran, S. Al-Ahmadi, H. Yanikomeroglu, and S. M. Sait, “A survey of rate-optimal power domain NOMA with enabling technologies of future wireless networks,” *IEEE Commun. Surv. Tutor.*, vol. 22, no. 4, pp. 2192–2235, 4th Quart. 2020.
- [140] V. Niemela, J. Haapola, M. Hamalainen, and J. Iinatti, “An ultra wideband survey: Global regulations and impulse radio research based on standards,” *IEEE Commun. Surv. Tutor.*, vol. 19, no. 2, pp. 874–890, 2nd Quart. 2017.
- [141] M. Kordestani, A. A. Safavi, and M. Saif, “Recent survey of large-scale systems: Architectures, controller strategies, and industrial applications,” *IEEE Syst. J.*, vol. 15, no. 4, pp. 5440–5453, Dec. 2021.
- [142] K. Wu, J. A. Zhang, X. Huang, and Y. J. Guo, “Frequency-hopping MIMO radar-based communications: An overview,” *IEEE Aerosp. Electron. Syst. Mag.*, vol. 37, no. 4, pp. 42–54, Apr. 2022.
- [143] H. Zhang, B. Di, K. Bian, Z. Han, H. V. Poor, and L. Song, “Toward ubiquitous sensing and localization with reconfigurable intelligent surfaces,” *Proc. IEEE*, vol. 110, no. 9, pp. 1401–1422, Sep. 2022.
- [144] G. Gradoni, M. Di Renzo, A. Diaz-Rubio, S. Tretyakov, C. Caloz, Z. Peng, A. Alu, G. Lerosey, M. Fink, V. Galdi *et al.*, “Smart radio environments,” *arXiv preprint arXiv:2111.08676*, Nov. 2021.
- [145] O. Maraqa and T. M. N. Ngatched, “Optimized design of joint mirror array and liquid crystal-based RIS-aided VLC systems,” *IEEE Photonics J.*, vol. 15, no. 4, pp. 1–11, Aug. 2023.
- [146] ITU-R, Report M.2516-0, *Future Technology Trends of Terrestrial International Mobile Telecommunications Systems Towards 2030 and Beyond*, Nov. 2022. [Online]. Available: <https://www.itu.int/pub/R-REP-M.2516-2022>
- [147] R. Liu, S. Zheng, Q. Wu, Y. Jiang, N. Zhang, Y. Liu, M. Di Renzo *et al.*, “Sustainable wireless networks via reconfigurable intelligent surfaces (RISs): Overview of the ETSI ISG RIS,” *arXiv preprint arXiv:2406.05647*, Jun. 2024.
- [148] ETSI, Report ETSI.GR.RIS.002 V1.1.1, *Reconfigurable Intelligent Surfaces (RIS): Technological Challenges, Architecture and Impact on Standardization*, Aug. 2023. [Online]. Available: [https://www.etsi.org/deliver/etsi\\_gr/RIS/001\\_099/002/01.01.01\\_60/gr\\_ris002v010101p.pdf](https://www.etsi.org/deliver/etsi_gr/RIS/001_099/002/01.01.01_60/gr_ris002v010101p.pdf)